CONTRACTOR REPORT

SAND88-8100
UC-62a
Unlimited Release

Central Receiver Plant Evaluation IV) Themis Thermal Storage Subsystem Evaluation

Ecole Centrale des Arts et Manufactures
Geser Group: A. Amri, M. Izygon, B. Tedjiza
Program Manager: C. Etievant
France

Prepared by Sandia National Laboratories, Albuquerque, New Mexico 87185
and Livermore, California 94550 for the United States Department of Energy
under Contract DE-AC04-76DP00789

Printed February 1988

Issued by Sandia National Laboratories, operated for the United States Department of Energy by Sandia Corporation.

Printed in the United States of America
Available from
National Technical Information Service
5285 Port Royal Road
Springfield, VA 22161

NTIS price codes
Printed copy: A05
Microfiche copy: A01

UC-62a

SAND88-8100
Unlimited Release
Printed February 1988

CENTRAL RECEIVER PLANT EVALUATION

IV) THEMIS THERMAL STORAGE SUBSYSTEM EVALUATION

December 1985

Prepared for SANDIA NATIONAL LABORATORIES
under contract n°90-1575
GESER GROUP: A.AMRI,M.IZYGON,B.TEDJIZA
Program Manager: C.ETIEVANT

Programme d'Evaluation AFME-CEA-ECP
ECOLE CENTRALE des ARTS et MANUFACTURES
Grande Voie des Vignes
92290 Châtenay-Malabry FRANCE

SANDIA NATIONAL LABORATORIES
Livermore ,California 94550 USA

ABSTRACT

This report presents an evaluation of the salt thermal storage subsystem of THEMIS. A description of the thermal storage subsystem is given and the operation procedures are presented.

The heat losses of the system are evaluated on the basis of cool-down experiments. The heat losses are then checked with the ones deduced from analytical models. The efficiency of the heat storage for a daily complete charge/discharge cycle is estimated to 95%.

The thermal storage behaviour is then described and analyzed over a complete day of actual operation.

Finally the maintenance activity during two years of operation are listed and some remarks are made on salt corrosion, salt stability and the lessons learned by the construction and operation of this system.

ACKNOWLEDGMENTS

This work was jointly supported by Commissariat à l'Energie Atomique (CEA).Agence Française pour la Maitrise de l'Energie (AFME). Ecole Centrale de Paris (ECP). Centre National de la Recherche Scientifique (CNRS-PIRSEM), and by the Sandia National Laboratories (SNL) under contract n° 90-1575.

The authors express their thanks to M.B. Rivoire and the GEST team, to M. J. Guilllard and the EDF G.R.P.T. team, to M. R.Genier and the EDF D.E.R. team for fruitful discussions on THEMIS evaluation.

FOREWORD

This document was prepared with funding from the U.S. Department of Energy's (DOE) Solar Thermal Technology Program. The goal of the Solar Thermal Technology Program is to advance the engineering and scientific understanding of solar thermal technology, and to establish the technology base from which private industry can develop solar thermal power production options for introduction into the competitive energy market.

Solar thermal technology concentrates solar radiation by means of tracking mirrors or lenses onto a receiver where the solar energy is absorbed as heat and converted into electricity or incorporated into products as process heat. The two primary solar thermal technologies, central receivers and distributed receivers, employ various point and lines-focus optics to concentrate sunlight. Current central receiver systems use fields of heliostats (two-axis tracking mirrors) to focus the sun's radiant energy onto a single tower-mounted receiver. Parabolic dishes up to 17 meters in diameter radiant energy onto a receiver. Troughs and bowls are line-focus along their focal lines. Concentrating collector modules can be used alone or in a multi-module system. The concentrated radiant conversion absorbed by the solar thermal receiver is transported to the conversion process by a circulating working fluid. Receiver temperatures range from 100°C in dish and central receiver systems.

The Solar Thermal Technology Program is directing efforts to advance and improve promising system concepts through the research and development of solar thermal materials, components, and subsystems, and the testing and performance evaluation of subsystems and systems. These efforts are carried out through the technical direction of DOE and its network of national laboratories who work with private industry. Together they have established a comprehensive, goal directed program to improve performance and provide technically proven options for eventual incorporation into the Nation's energy supply.

To be successful in contributing to an adequate national energy supply at reasonable cost, solar thermal energy must eventually be economically competitive with a variety of other energy sources. Components and system-level performance targets have been developed as quantitative program goals. The performance targets used in planning research and development activities, measuring progress, assessing alternative technology options, and making optimal component developments. These targets will be pursued vigorously to insure a successful program.

The work presented in this report was performed as part of the International subelement of the Central Receiver Systems task (Task 9). This work provides information for comparing the operational and design experiences of the French Central Receiver Project to those of the United States and other countries.

TABLE OF CONTENTS

ILLUSTRATIONS.

TABLES

REFERENCES

[1] J. HILLAIRET. La Centrale Solaire THEMIS 2500 KW . ENTROPIE N°103.1982 p 6.9

[2] X.POUGET ABADIE . Note de fonctionnement 1 FKH Stockages chaud et froid. Générateur de vapeur. Préparation du sel. Remplissage. Vidange. EDF.REAM.STG17 FKH000.

[3] B. RIVOIRE. Analyse des pertes thermiques du stockage. Note GEST0585. 27.02.85.

[4] R. GENIER.Mesures de niveau des réservoirs de stockage de sels fondus. EDF.DER.P52D83.81.30. 1981.

[5] R. GENIER. Réservoirs de stockage de sels fondus de la centrale solaire THEMIS. Résultats d'essais de mesure de niveau par bulle à bulle. EDF.DER.P52.D83.21. Mars 1983.

[6] A. RAYMOND. Etude de l'évolution de l'énergie stockée dans les réservoirs de THEMIS. EDF.DER.P52D19.54.85. Juillet 1985.

[7] P. SPITERI. Stability of salt and corrosion resistance of circuit materials in the THEMIS power plant. THERMO-MECHANICAL SOLAR POWER PLANTS Séries B. vol 2. D. REIDEL PUBLISHING Co.. June 1984.

1.0 INTRODUCTION

One of the main features of the THEMIS plant is the use of molten salt technology. Molten salt (Hitec: KNO_3 ,53%:$NaNO_2$,40 %:$NaNO_3$, 7%) is the medium used for both purposes of heat transfer and thermal storage.

This technology is expected to provide higher thermal storage efficiency, quicker start-up and easier plant control than water-steam systems.

The thermal storage subsystem is inserted in the primary salt loop as shown in Figures 1 and 2.

The thermal storage subsystem (FKH) is essentially composed of two tanks : the cold tank (FKH001BA) and the hot tank (FKH002BA). Two cold pumps (FRS001PO and FRS002PO) ensure the circulation of the molten salt from the cold tank to the hot tank through the solar receiver in normal operation of the latter.

Two hot pumps (FKH001PO and FKH002PO) ensure the circulation of the molten salt from the hot tank back to the cold tank through the steam generator while in energy production operation of the plant. A detailed description of the thermal storage subsystem of THEMIS is given in Section 2 of this report.

The operating modes of the thermal storage subsystem are described in Section 3.

The measuring methods used for the evaluation of the thermal storage performance are described in Section 4.

The experimental results collected during the cool-down tests of the thermal storage tanks are given in Section 5. and an evaluation of the heat loss of the system is deduced from these measurements.

Section 6 presents the heat loss results deduced from models of the thermal storage subsystem. The theoretical results of this section are compared with the experimental data of the previous section. An illustration of the actual thermal storage subsystem behaviour is presented in Section 7 where a complete typical day of operation is described and analyzed. The thermal storage subsystem efficiency is estimated in Section 8 for a complete charge-discharge daily cycle. The energy used to activate the thermal storage subsystem at its operating temperature is evaluated in Section 9.

An infra-red inspection of the heat storage components has been performed for heat loss evaluation. The conclusions of this test are presented in Section 10.

The lessons learned in operating and maintaining the molten salt thermal storage subsystem are presented in Section 11. Some remarks on the corrosion problems are made in Section 12.

Our conclusions on the choice of the molten salt technology for the thermal storage subsystem are presented in Section 13.

2.0 THERMAL STORAGE SUBSYSTEM DESCRIPTION

The thermal storage subsystem of THEMIS has been designed for 5 hours of operation of the plant with an output of 2.200 kWe in the thermal storage discharge mode.

To ensure this output, an input of heat of 8.000 kWth is required into the steam-generator. Assuming a hot salt temperature of 450°C and of 250°C, we have a 200° salt temperature variation in the steam-generator. With Cp = 1.561 kJ kg°C, the corresponding enthalpy change of the salt is 312.2 kJ/kg (0.0867 kWh/kg). The total amount of hot salt required in the hot tank when fully charged is 462.000 kg. The total amount of salt in the primary loop is slightly larger : 537.000 kg. Therefore,the two tanks constituting the thermal storage subsystem have a capacity of 310 m^3 each.

The thermal storage subsystem can be considered as the interface of the solar receiver subsystem FRS with the steam-generator GPV001GV. The connections of the thermal storage tanks with these two subsystems are shown in Figures 1 and 2. Figure 2 shows also the connections of the cold tank with part of the storage auxiliary equipment including the salt melting tank FKH00 3BA and the drain tank FKH004BA.

The thermal storage subsystem equipment is installed in the machine hall between levels 0.00m and + 10.3m as shown in Figure 3.

Both storage tanks are cylindrical. They are placed side by side at level 0.00m with their axis oriented North to South.

The two hot pumps feeding the steam generator and the two cold pumps feeding the solar receiver are placed inside the hot tank and the cold tank respectively. They are coupled by a shaft to their drive-motors placed at the top of the tanks at level − 7.00m.

The steam generator is cylindrical. It is placed above and between the two storage tanks, just below level − 7.5m.

The equipment for salt handling and melting is located in the north-east section of the mahine hall. The melting tank is placed at level − 7.00m.

The drain tank and its pump are placed at level 0.00m, just in between the two storage tanks. The flaking machine is placed at level + 4.00m, east of the machine hall.

The specifications of the main components of the thermal storage subsystem are given below.

2.1 THERMAL STORAGE TANKS

Both thermal storage tanks FKH001BA and FKH002BA are identical. They only differ by the type of steel used for the vessel. Figure 4 shows one of these tanks.

Each tank is supported by four supports, one fixed and three free to slide to allow thermal expansion. The sliding supports are equipped with "Klingerflon Duplex" sliding blocks having a friction coefficient of 0.04. Additional "Marinite 45" heat insulators protect the sliding blocks against unsafe temperatures (maximum temperature allowed 50°C).

The thermal storage tank manufacturer is CFEM (Compagnie Française d'Entreprises Metalliques).

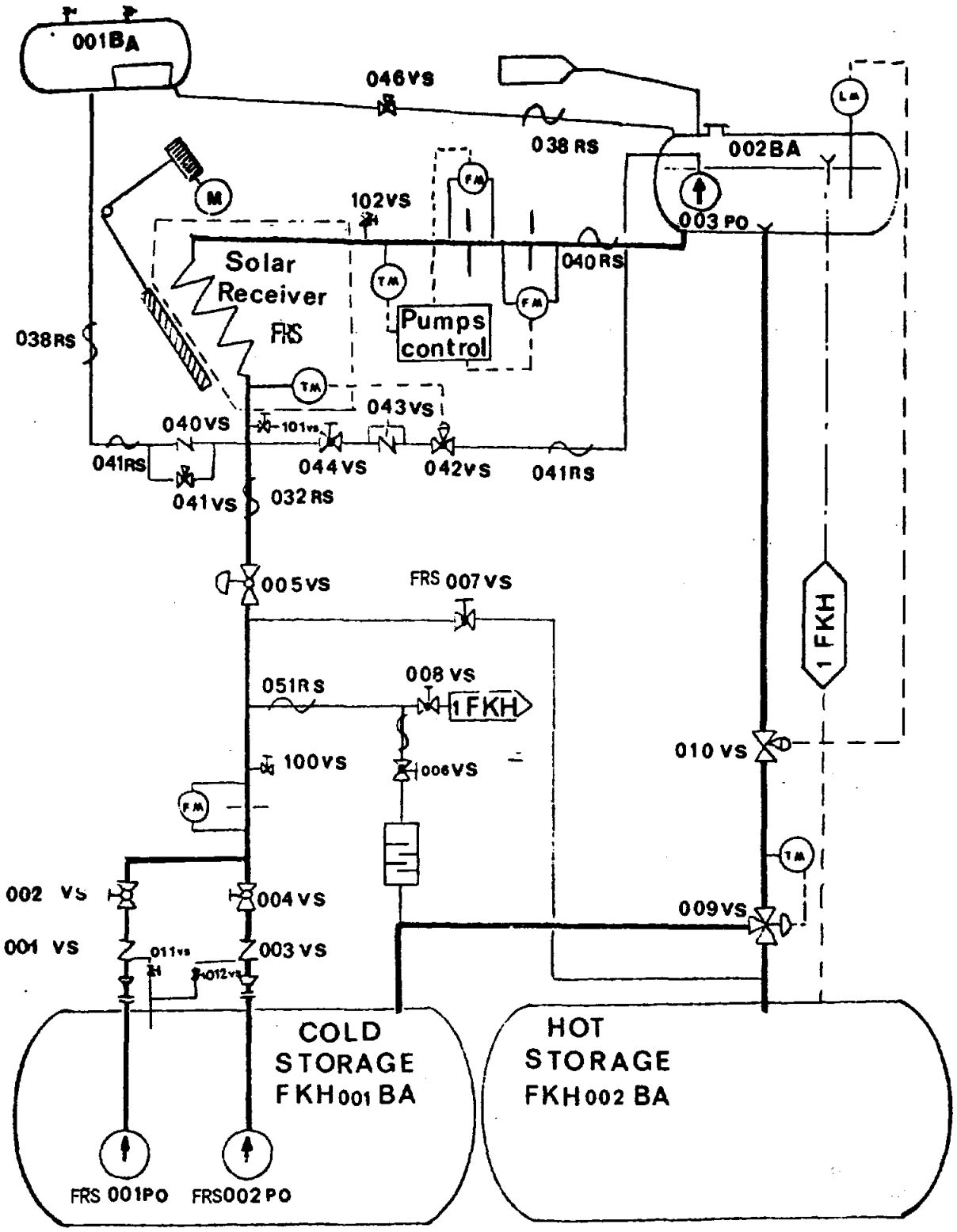

FIG 1 : THERMAL STORAGE SUBSYSTEM (FKH) CONNECTIONS WITH THE SOLAR RECEIVER SUBSYSTEM (FRS)

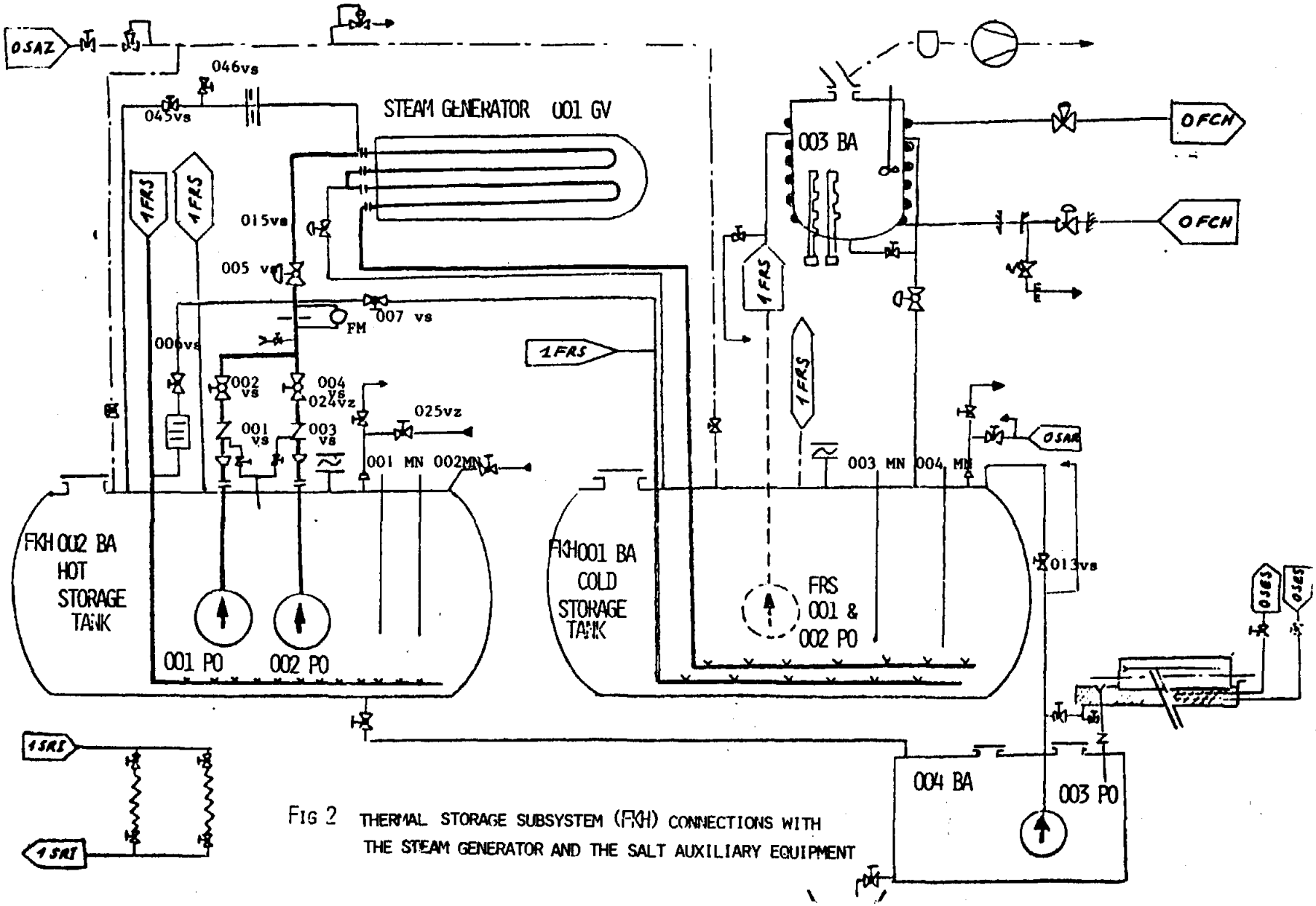

FIG 2 THERMAL STORAGE SUBSYSTEM (FKH) CONNECTIONS WITH THE STEAM GENERATOR AND THE SALT AUXILIARY EQUIPMENT

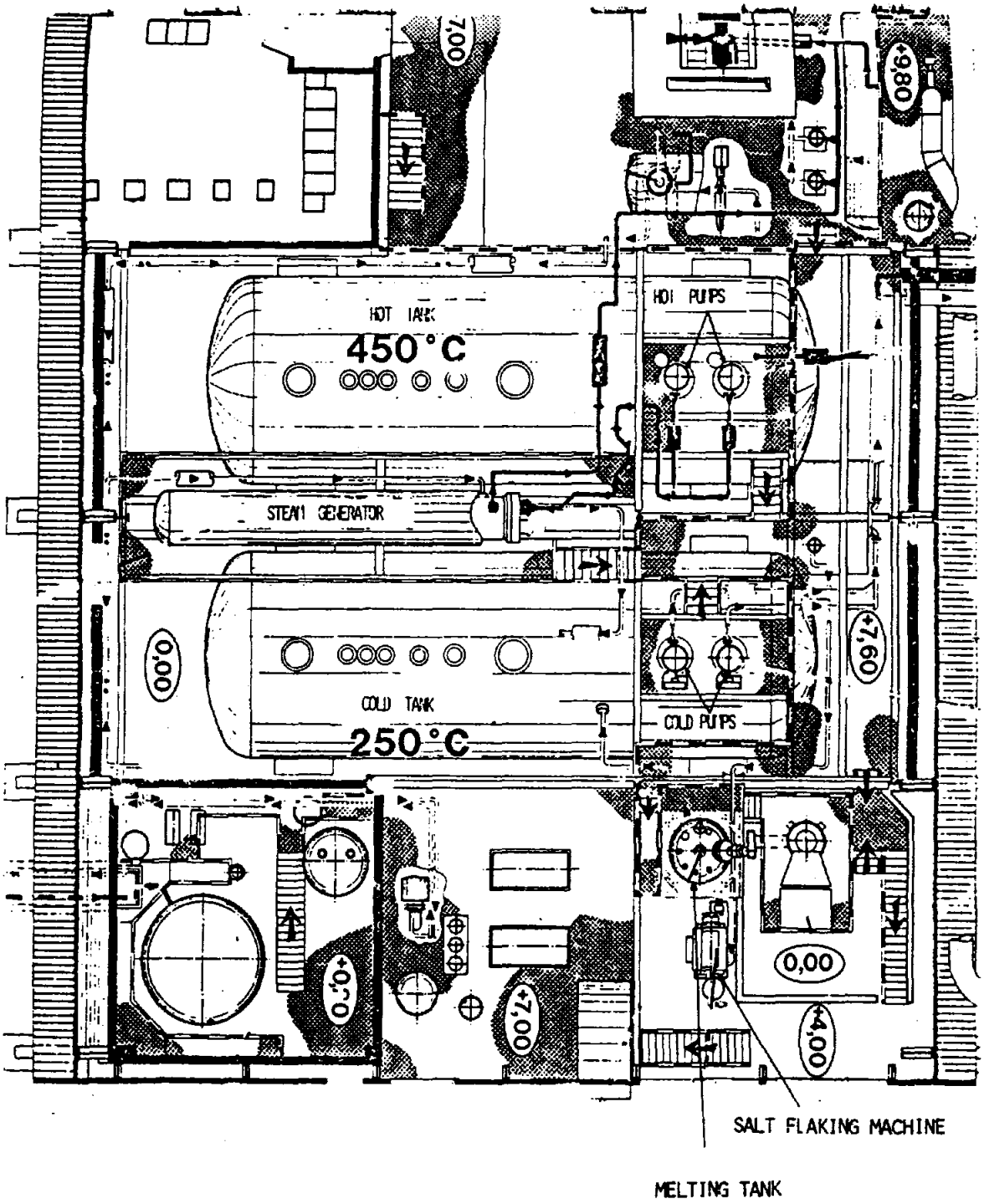

FIGURE 5 : THERMAL STORAGE SUBSYSTEM LAYOUT

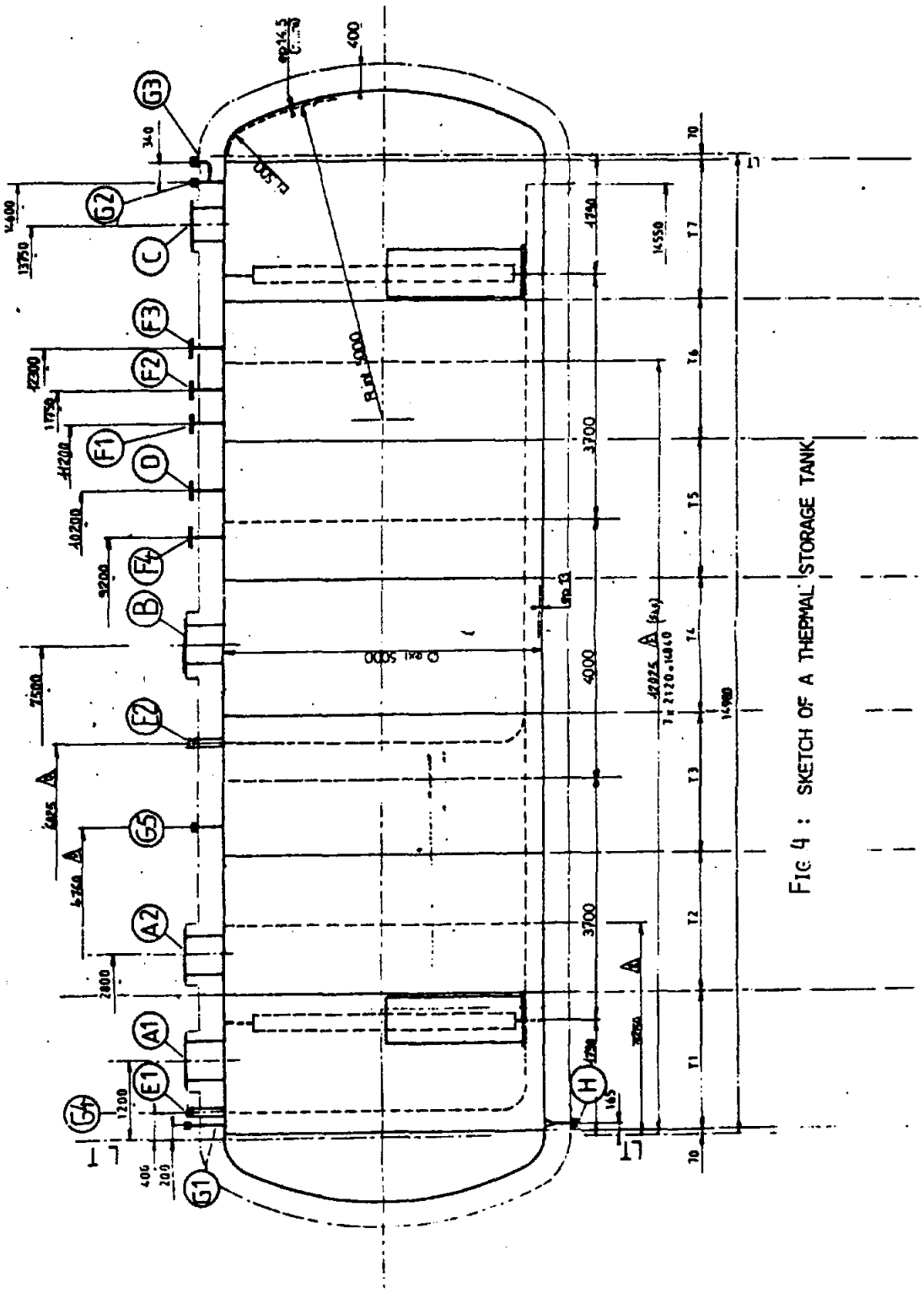

FIG 4 : SKETCH OF A THERMAL STORAGE TANK

TABLE 2-1

THERMAL STORAGE TANK SPECIFICATION

	Cold Tank FKH001BA	Hot Tank FKH002BA
Length m	16.940	16.940
Diameter m	5	5
Volume m^3	310	310
Shell thickness mm	13	13
Type of steel	A42CP	15CD205
Design Temp.°C	250	450
Max.Salt Temp.°C	400	480
Max.Salt Pres. bar	3 + salt hydro.pres.	3 + salt hydro.pres.
Max.depress.bar	0.5	0.5
Vessel weight kg	40000	40000
Salt weight contained kg	537000	537000
Insulation kg	15800	15800
Insulation thickness mm	400	400
Weight of motor driven pumps kg	3000	3000
Additional weight kg	9000	9000
Total weight of one full tank with equipment kg	564800	564800

2.2 MOTOR DRIVEN PUMPS

Hot pumps FKH001PO and FKH002PO

The two hot pumps are placed at the bottom interior of the hot tank, just above the fixed tank support. These pumps are a centrifugal type with a vertical axis. The two drive motors are placed out of the tank, above the pumps to which they are coupled by a 5 m vertical shaft made of three sections (one of 1.8 m and two of 1.6 m). The pumps are manufactured by "Rheinhutte" and the drive motors by "Jeumont Schneider".

The two hot pumps are equipped with a 2 kW oil preheating device, made of 3 resistors of 660 W each, star connected. A thermostat is used in this device to disconnect the motors from their power supply as long as the operating temperature of the pumps has not been reached.

The specification of the hot motor driven pumps is given in Table 2-2.

TABLE 2-2

MOTOR DRIVEN HOT PUMP SPECIFICATION

	Unit	Minimum	Design	Maximum
Salt Inlet Temp.				
normal	°C	450	450	450
min.	°C	250	250	250
max.	°C	470	470	470
Flow rate	kg s	0	25.63	29.48
Total pumping height		8	45	60
Shaft power	kW	1.4	24.6	36.9
Pump efficiency	%		46	47
Pump speed with				
normal flow rate	R.P.M		1760	2020
zero flow rate	R.P.M	750		
Drive motor power	kW			40.5

Cold pumps FRS001PO and FRS002PO

These two pumps belong by convention to the solar receiver subsystem FRS and are. therefore. described in the solar receiver evaluation report.

Drain pump FKH003PO

When in exceptional circumstances the thermal storage tanks have to be completely emptied. the remaining salt in the dead volume of the tank can be drained by gravity into the drain tank FKH004BA. The drain pump FKH003PO can then be used to pump the salt from this tank either to the flaking machine or back to the cold storage tank FKH001BA.

The specification of the drain pump FKH003PO is given in Table 2-3.

TABLE 2-3

DRAIN PUMP FKH003PO

	Units	Specification
Salt inlet temperature	°C	250
Salt Flow rate(weight)	kg/s	3.5
Salt Flow rate(volume)	m^3/h	2
Total pumping height		
at normal flow rate	MPa	0.186
at zero flow rate	MPa	0.186
Pump speed	R.P.m	1450
Drive motor power	kW	0.73

2.3 STEAM GENERATOR

The steam generator is manufactured by C.I.T.E.C.. It is heated by the hot salt . It performs the three functions of preheating, vaporizing the feed water and superheating the steam .

As a convenience for construction, the steam generator is placed between the two thermal storage tanks as shown in Figure 3.

The steam generator vessel is a horizontal cylinder . It contains two U shaped banks of tubes, inside which the hot salt circulates. One of these banks, the preheating and vaporizing section. is immersed in the feed-water that fills half the vessel. The other bank of tubes, the superheating

section, is placed in the upper part of the vessel filled with the steam generated in the lower section.

The two banks of tubes are connected by a U shaped connection piece trace heated by electricity and drained by the valve FKH015VS.

The steam generator axis is slightly inclined so as to allow draining by gravity. The steam-generator specification is given in Table 2-4.

TABLE 2-4

STEAM GENERATOR SPECIFICATION

TUBES

Metal		15 CD 205
Number of tubes per bank:		
Superheating section		105
Preheating and vaporizing section		122
Tube diameter	mm	14
Tube thickness	mm	1.5
Tube maximum internal pressure	bar	10
Tube maximum temperature	°C	450
Heat exchange surface:		
Superheating section	m^2	89.9
Preheating and vaporizing section	m^2	103.9

STEAM GENERATOR VESSEL

Diameter	m	1.2
Lenght	m	12
Volume of water in the preheating and vaporizing section	m^3	5

HOT SALT SIDE

		design point	**maximum**	**1/3 load**
Inlet salt temp.	°C	450	450	450
Outlet salt temp. Superheating section	°C	406.6	407.7	402.1
Outlet salt temp. Boiler section	°C	260.7	266.6	237.4
Outlet salt temp. Preheating section	°C	244.9	251.2	215.3
Salt flow rate	kg/s	25.35	28.34	7.17
Power exchanged	kW	8116	8793	2625

WATER-STEAM SIDE

Steam pressure	bar	42.2	46.42	30
Super heated steam temp.	°C	445.3	444.7	448.6
Feed water flow rate	kg/s	3.312	3.643	0.99

2.4 SALT FILLING EQUIPMENT

The filling of the cold tank FKH001BA with salt is a long operation lasting about 20 working days (8 hours a day). The filling equipment is sized to melt 3000 kg of salt per hour (50 kg per minute).

The filling equipment (Figure 5) is composed of

- a clod breaking machine located at level 0.00 m.
- a bucket conveyor carrying the salt up to level + 7.00 m.
- a melting tank FKH003BA heated either by thermal oil circulation (Gilotherm TH heated by the parabolic dishes), or by electrical resistors.

The melting tank specification is given below :

MELTING TANK (FKH003BA) SPECIFICATION

Volume	m^3	4.00
Weight	kg	2000.
Salt capacity	kg	12000.
Max. Temperature	°C	350
Max. Pressure	bar	1

For a salt melting rate of 3 000 kg/h at 220°C, the specification of the Gilotherm heating system is the following :

Inlet Gilotherm temperature	°C	320
Outlet Gilotherm temperature	°C	200
Power exchanged	kW	350
Gilotherm flowrate	m^3/h	5.186

Electrical heating is used to start the salt melting. This is done by 18 electrical resistors of 5.56 kW each. These resistors are of cylindrical shape (Length 1.65 m. Diameter 0.057 m).

The melting tank is also equipped with a propeller mixer, driven by a 5.5 kW electrical motor and a radial fan driven by a 0.12 kW electrical motor.

2.5 SALT DRAINING EQUIPMENT

On special occasions, chemical composition control for instance, some salt has to be extracted from the system. This salt is pumped out and cooled down and then solidified in flakes, ready to be stored in bags.

The main equipment for this procedure is the flaking machine. It is composed of a rotating water-cooled drum on the surface of which the molten salt is solidified in flakes and then conveyed to a funnel for bagging.

This machine has a processing capacity of 500 kg of salt per hour. The temperature of the salt flakes is 75°C maximum. The water flow rate necessary for cooling the drum is 4 m^3/h.

The pieces of equipment for salt handling, filling and draining have been manufactured by BERTRAMS.

2.6 TRACE HEATING OF THE THERMAL STORAGE EQUIPMENT

A pressurized water network of pipes is used for trace heating the following thermal storage equipment :

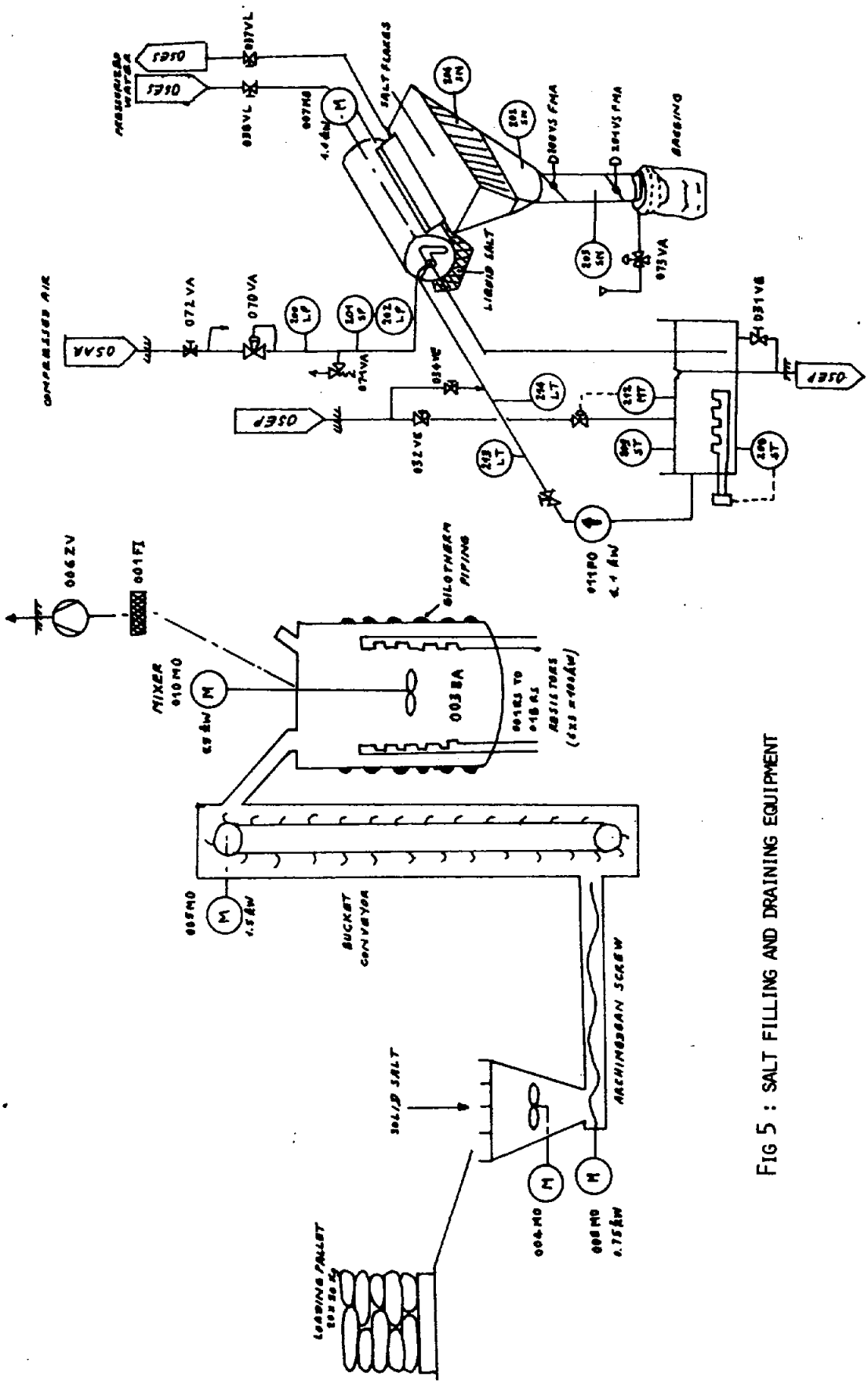

FIG 5 : SALT FILLING AND DRAINING EQUIPMENT

- Cold tank
- Hot tank
- Steam generator loop
- Solar receiver loop (the receiver itself is electrically trace heated)
- Auxiliary loops of the filling and draining systems

The trace heating pressurized water (250°C, 55 bar) is heated either by heat exchange with the Gilotherm loop of the parabolic dishes (Figure 6) or by electrical heating by means of a 150 kW resistor SES001RE (Figure 7).

The ultrasonic flowmeter velocimeter FKH001MD and the drain tank FKH004BA are electrically trace heated.

The pressurized water network is designed to heat :

- the salt pipes and accessories : valves,insulation.. from 10°C up to 220°C in 12 hours maximum;
- the hot tank and the cold tank for the first start up. from 10°C up to 220°C in 72 hours.

The corresponding power delivered by the pressurized water trace heating system breaks down as follows

	Power (kW)
.Receiver loop (FRS)	
-Riser	20
-Downcomer	30
-Other (FRS) salt pipes	26
.Steam-generator loop	7
.Other FKH piping,melting tank. flaking machine...	28
TOTAL	111

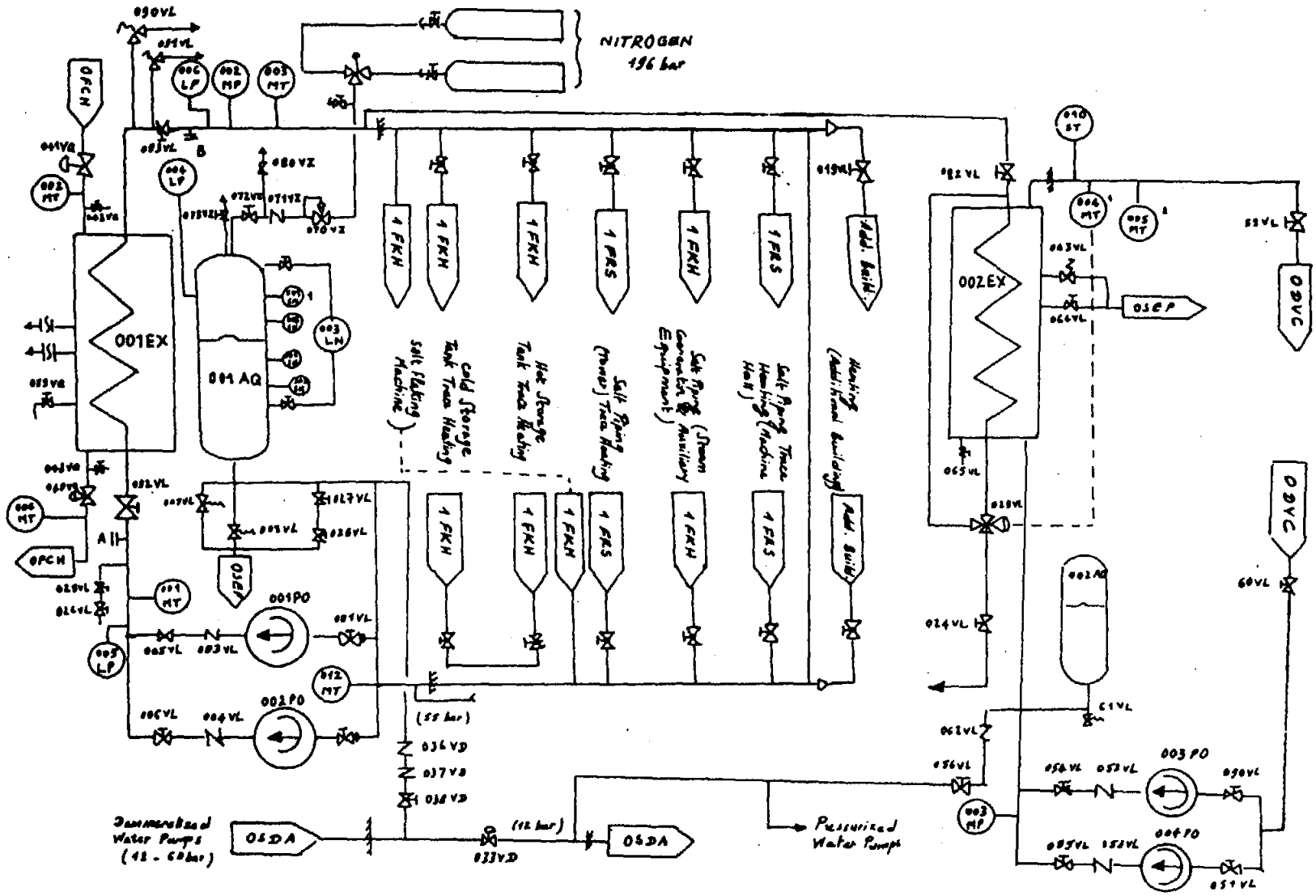

FIG 6 : PRESSURIZED WATER TRACE HEATING

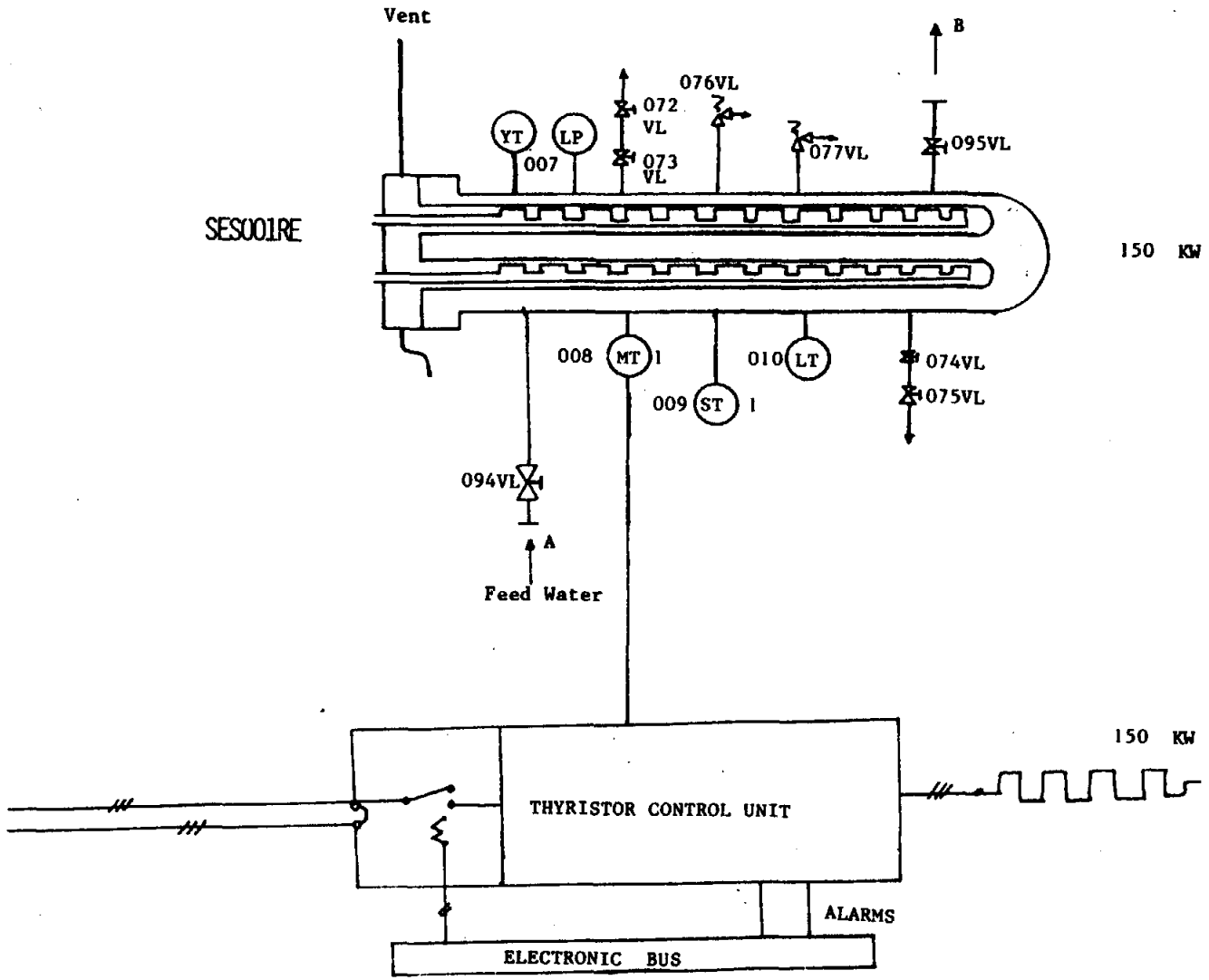

FIG 7 : ELECTRIC HEATER

3.0 THERMAL STORAGE OPERATION

3.1 NORMAL OPERATION

In normal operation of the plant. there are two modes of operation that can occur either simultaneously or time shifted. These two modes are :

- The thermal storage charge mode :

In this mode the salt is pumped from the cold tank to the hot tank through the receiver. This operation can occur during all the sunshine hours. i.e about 8 hours per clear day on average.

- The thermal storage discharge mode :

In this mode the salt is pumped from the hot tank to the cold tank through the steam generator. The duration of this operation depends on the energy production program of the plant.

These two modes are almost totally decoupled in time. They should of course overlap every time it becomes necessary to limit the energy input into the hot tank. whose maximum thermal storage capacity is 40 MWH.

During operation. the levels of molten salt in the two tanks vary slowly.They can even stay stationnary when the flowrates in the receiver loop and in the steam generator loop are balanced.

During operation. the nitrogen differential pressure between both tanks is limited within a range of 0.5 bar.

In the charge mode. the salt temperature in the hot tank is kept constant at about 400°C. In the cold tank. temperature variations may occur. depending on the salt outlet temperature from the steam generator and on the salt outlet temperature from the receiver in the recycling mode. In this latter case whenever the outlet temperature does not reach a threshold ranging between 350 and 400°C. the salt is sent back to the cold tank (recycling). In normal operation the salt temperature in the cold tank is not supposed to deviate very much from 250°C. This value of 250°C will be considered as the reference temperature for evaluating the available heat in the thermal storage subsystem.

3.2 NORMAL START-UP AND SHUTDOWN

Long shutdown (more than 7 days)

For long shutdown periods. the salt from all equipment is drained to the cold tank. When all the salt is in the cold tank at 250°C. it takes 30 days to cool down to 200°C. When this temperature is reached. further cooling should be avoided. Salt heating should then be started by use of either the salt melting equipment or the pressurized water trace heating system.

Short shutdown (a night or a few days)

During short shutdown periods. the solar receiver is not drained and the pumps FRS001PO and FRS002PO are kept available to circulate salt from the cold tank to prevent salt freezing in the receiver loop.

Similarly the steam generator is not drained. neither on the salt side, nor on the water side. The hot pumps FKH001PO and FKH002PO are kept available and circulate pulses of salt in order to keep the steam generator temperature above 250°C.

Steam generator start- up

Starting up the steam generator from cold initial conditions requires the following procedure:

The salt loop of the steam generator is heated up to the temperature of 220°C in 12 hours. This is done by opening the valves allowing pressurized water circulation in the trace heating

pipes. When all the components of the salt loop of the steam generator have reached 220°C, the pressurized water pipes are drained in order to prevent excessive pressure rise up.

Then the hot pump FKH001PO or FKH002PO is started at reduced speed. The salt flow rate is limited to 5% of its nominal value in order to prevent thermal shock of the steam generator tubes. As soon as the temperature reaches 300°C at the outlet of the superheating section, where the temperature is measured by the thermocouple GPV102MT, the salt flow rate is gradually increased up to its working value.

Hot steam generator shutdown

Hot steam generator shutdown can be started by turbine trip or by other causes. Then the hot salt pumps are slowed down and the salt flow rate is reduced to zero.

Steam generator draining is then started when the salt pumps have completely stopped.

3.3 SPECIAL OPERATION OF THE THERMAL STORAGE SUBSYSTEM

There are some other operation modes of the thermal storage subsystem that are specified for special occasions. These modes are not described here but are discussed in the EDF document : Ref '2'.

These special modes are :

- Salt circulation through a flow limiter.
- Extraction and refueling for salt regeneration.
- First filling of the thermal storage tanks.
- Operation in case of steam generator tube break.
- Operation in case of thermal storage tank outage.

3.4 USE OF THE COLD TANK FOR SUPPLYING HEAT TO THE PRESSURIZED WATER TRACE-HEATING SYSTEM

In Section 2-6, the thermal storage trace heating equipment was described. The pressurized water trace heating piping was initially designed to be heated either by the Gilotherm from the parabolic dishes or by electrical heating by means of the 150 kW resistor SES001RE.

The Gilotherm loop became operational by the end of September 1985 and until then the use of the electric heating was a heavy burden in the parasitics balance.

A third method for heating the pressurized water circuit turned out to be both practical and energy efficient. It consists in using the eight trace heating pipes placed on the external face of the cold tank, as a heat source for the pressurized water circuit. This mode of trace heating can be operated by acting on valves FKH010VL and FKH009VL shown in Figure 6.

pipes. When all the components of the salt loop of the steam generator have reached 220°C, the pressurized water pipes are drained in order to prevent excessive pressure rise up.

Then the hot pump FKH001PO or FKH002PO is started at reduced speed. The salt flow rate is limited to 5% of its nominal value in order to prevent thermal shock of the steam generator tubes. As soon as the temperature reaches 300°C at the outlet of the superheating section, where the temperature is measured by the thermocouple GPV102MT, the salt flow rate is gradually increased up to its working value.

Hot steam generator shutdown

Hot steam generator shutdown can be started by turbine trip or by other causes. Then the hot salt pumps are slowed down and the salt flow rate is reduced to zero.

Steam generator draining is then started when the salt pumps have completely stopped.

3.3 SPECIAL OPERATION OF THE THERMAL STORAGE SUBSYSTEM

There are some other operation modes of the thermal storage subsystem that are specified for special occasions. These modes are not described here but are discussed in the EDF document : Ref '2'.

These special modes are :

- Salt circulation through a flow limiter.
- Extraction and refueling for salt regeneration.
- First filling of the thermal storage tanks.
- Operation in case of steam generator tube break.
- Operation in case of thermal storage tank outage.

3.4 USE OF THE COLD TANK FOR SUPPLYING HEAT TO THE PRESSURIZED WATER TRACE-HEATING SYSTEM

In Section 2-6, the thermal storage trace heating equipment was described. The pressurized water trace heating piping was initially designed to be heated either by the Gilotherm from the parabolic dishes or by electrical heating by means of the 150 kW resistor SES001RE.

The Gilotherm loop became operational by the end of September 1985 and until then the use of the electric heating was a havy burden in the parasitics balance.

A third method for heating the pressurized water circuit turned out to be both practical and energy efficient. It consists in using the eight trace heating pipes placed on the external face of the cold tank, as a heat source for the pressurized water circuit. This mode of trace heating can be operated by acting on valves FKH010VL and FKH009VL shown in Figure 6.

4.0 DESCRIPTION OF THE MEASURING TECHNIQUES

The analysis of the heat loss and the energy balance of the thermal storage subsystem requires measurement of the following parameters :

- Salt flow at the inlet and the outlet of each tank.
- Salt temperature at the inlet and the outlet and at several points of both tanks.
- Salt level or salt volume in each tank.

The available equipment for providing these measurements is described below.

4.1 SALT FLOW MEASUREMENTS

There are two salt flowmeters that can be used for measuring the salt flow at the inlet and the outlet of the two tanks. These flowmeters FRS002MD and FKH001MD are located as shown in Figure 8.

FRS002MD is a Venturi nozzle placed on the riser at the solar receiver inlet.

FKH001MD is an ultrasonic flowmeter that measures the salt velocity by comparing the propagation time of ultrasonic pulses moving in a upstream and downstream direction.

It is seen in Figure 8 that FRS002MD measures the outlet flow Q_{OUTC} of the cold tank FKH001BA in normal operation . It also measures the recycling salt flow Q_{RECY} when TOR2 is in Position 0. It measures the inlet salt flow Q_{INH} into the hot tank FKH002BA when TOR2 is in Position 1.

In the same way FKH001MD measures the outlet salt flow Q_{OUTH} from the hot tank FKH002BA at any time. It measures the inlet salt flow Q_{INC} into the cold tank FKH001BA when TOR15 is in Position 0.

4.2 SALT TEMPERATURE MEASUREMENTS

Salt and metal temperatures are measured by thermocouples located at various places in the system.

Thermocouples used for temperature measurements in the hot tank FKH002BA . Metal temperature : There are 24 thermocouples (FKH001MT, FKH002MT....FKH024MT) that are placed on the vessel.They are regularly distributed along three circumferences C_1,C_2,C_3 as shown in Figure 9. Ten of these thermocouples (FKH001MT, FKH005MT, FKH009MT, FKH010MT, FKH012MT, FKH013MT, FKH014MT, FKH016MT, FKH017MT and FKH021MT), are permanently recorded by the data acquisition system AQMT.

Hot salt temperature : This temperature is measured by the thermocouple FKH401MT.

Temperature measurements in the cold tank FKH001BA : Metal temperature : there are 24 thermocouples, regularly distributed on the circumferences T_1, T_2, T_3 in three sections of the vessel.Ten of these thermocouples (FKH033MT, FKH034MT, FKH0036MT, FKH037MT, FKH038MT, FKH040 MT, FKH041MT, and FKH045MT), are permanently recorded by AQMT. The distribution of these sensors on the vessel is represented in Figure 10.

Cold salt temperature : This measurement is given by the thermocouple FKH402MT. The following temperatures of interest are also measured :

- Salt temperature at the steam generator inlet T_{INSG} measured by thermocouples FKH100MT and FKH101MT.

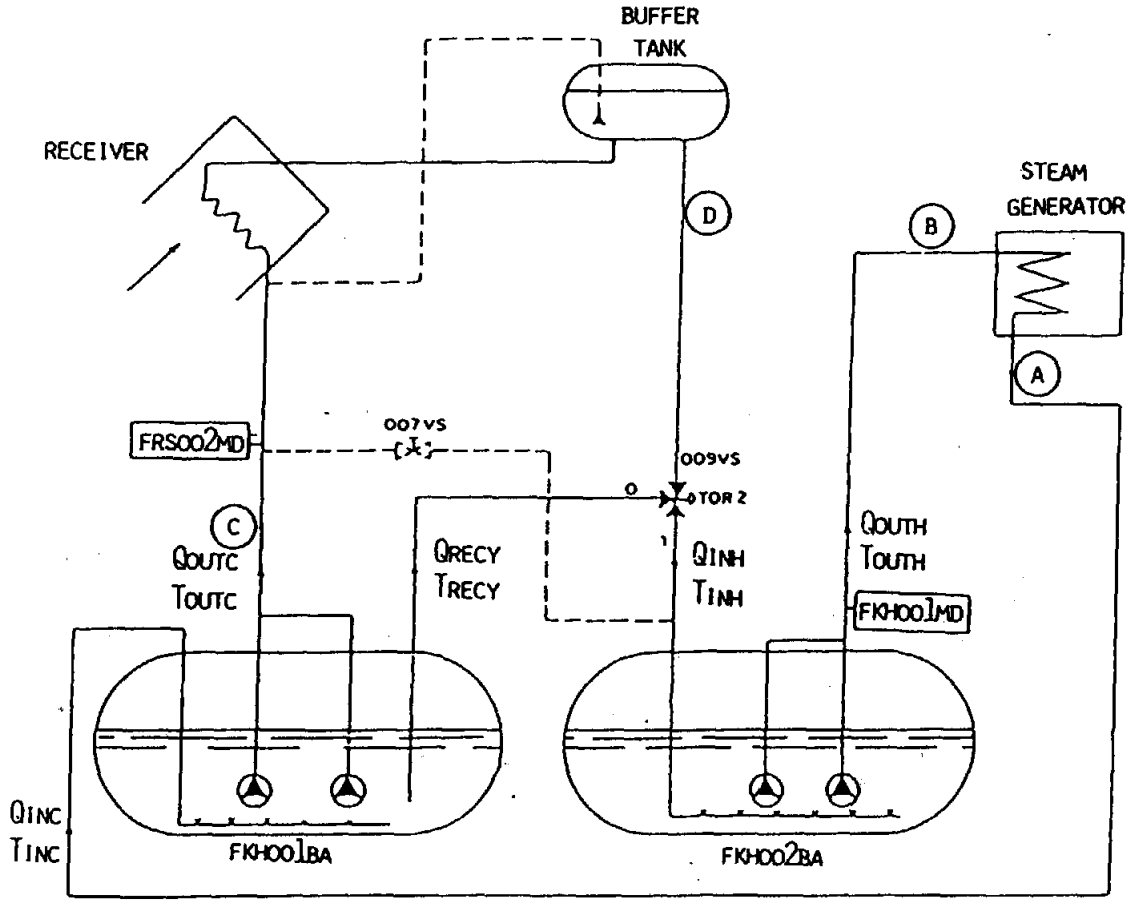

FIG. 8 LOCATION OF SENSORS USED FOR THERMAL STORAGE ENERGY BALANCE EVALUATION

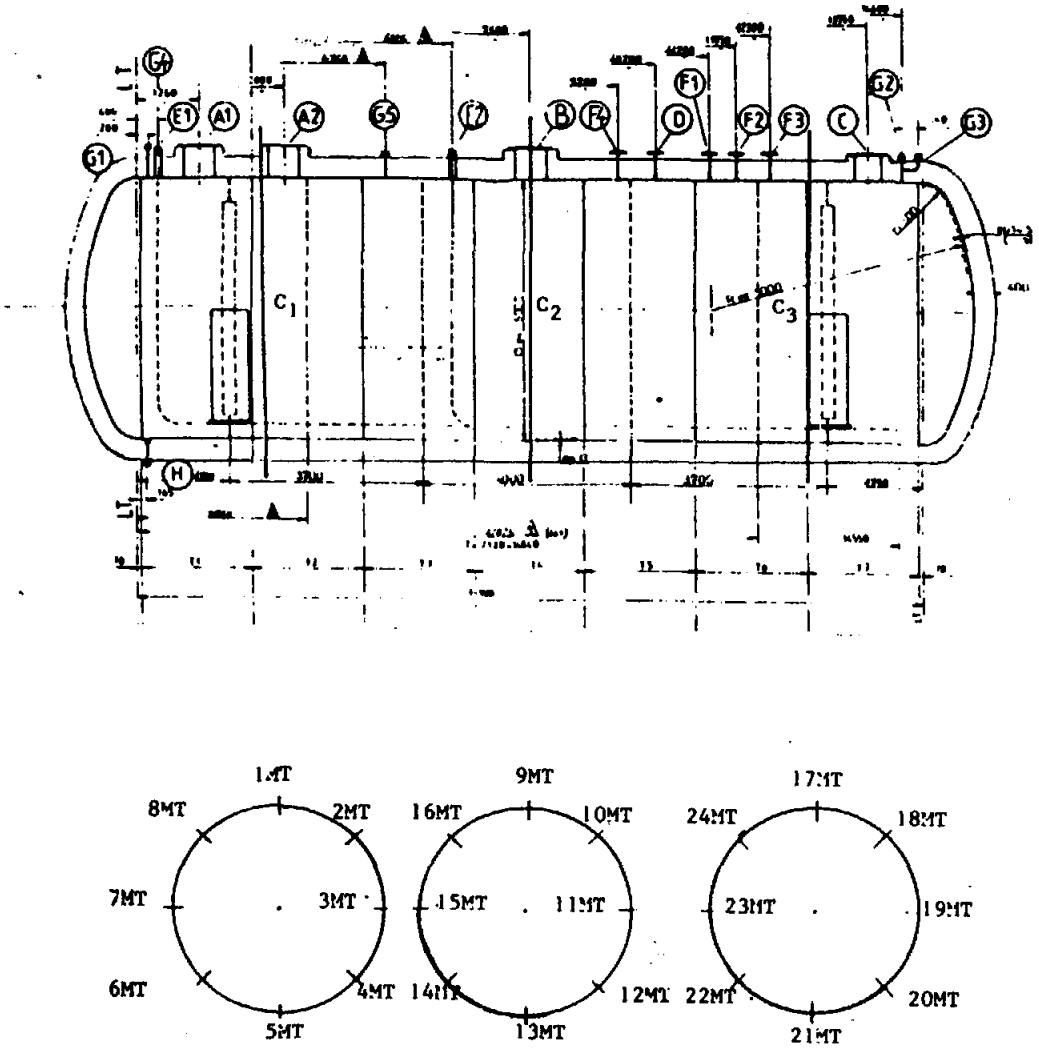

FIG 9 : THERMOCOUPLE DISTRIBUTION ON THE HOT TANK FKH 002BA

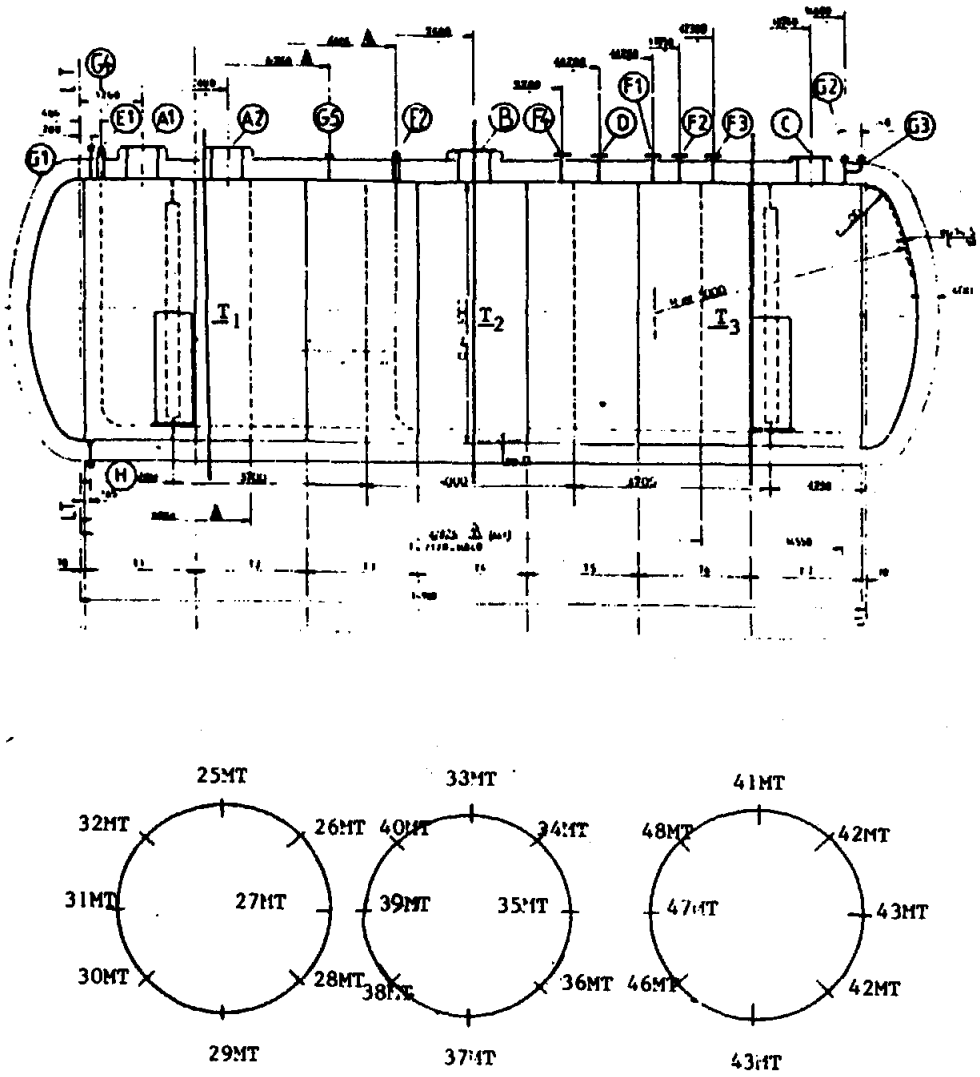

FIG 10 : THERMOCOUPLE DISTRIBUTION ON THE COLD TANK FKH 001BA

- Salt temperature at the steam generator outlet T_{OUTSG} measured by thermocouples FKH103MT and FKH104MT.
- Salt temperature at the solar receiver inlet T_{INSR} measured by thermocouples FRS200MT and FRS201MT.
- Salt temperature at the solar receiver outlet T_{OUTSR} measured by thermocouples FRS101MT and FRS102MT.

4.3 SALT LEVEL MEASUREMENTS

The salt levels in the hot tank and in the cold tank are derived from salt hydrostatic pressure measurements using a gas bubble generation technique. A vertical tube is introduced into the bulk of salt with one extremity at the bottom of the tank. A variable pressure of nitrogen is introduced into the tube. There is a pressure threshold for bubble formation. This pressure threshold is measured. The level of salt in the tank is then derived from the expression :

$$\Delta P = \rho_s g h$$

where :

- h: level of salt
- ρ_s : salt specific gravity (temperature dependent)
- ΔP : difference between the bubble threshold pressure and the nitrogen cover gas pressure.

In the hot tank there are two bubble pressure threshold sensors FKH001MN and FKH002MN, a nitrogen cover pressure sensor FKH008MP and a salt temperature sensor FKH401MT, that are used for the salt level determination. Similarly in the cold tank these measurements are made by two bubble pressure threshold sensors FKH003MN and FKH004MN, a nitrogen cover pressure sensor FKH007MP and a salt temperature sensor FKH402MT.

4.4 SALT VOLUME EVALUATION

Both tanks being geometrically identical, they are supposed to have the same salt level versus salt volume dependence. A calibration has been made at 15°C for FKH002BA, using water instead of salt. The calibration curve is represented in Figure 11. The data from this calibration are listed in Table 4-1.

This dependence has been approximated by Rivoire who proposed a 3rd degree polynomial:

$$V = -0.0026952\ h^3 + 1.997\ h^2 + 327.8\ h - 4650.$$

where V is in liters and h in centimeters.

This relationship gives the volume with an accuracy of 0.1 percent for 140 cm < h < 430cm and an accuracy of 0.5 percent for 60 cm < h < 450 cm.

The volume, level dependence having been calibrated at 15°C, a temperature correction has to be introduced to take into account the thermal expansion of the tank containing the salt at temperature T. The actual volume of salt is expressed by :

$$V_s(T) = V_{15}(1 + \alpha(T-15))^3$$

where α = linear metal dilatation coefficient.

$$\alpha = 1.13.10^{-5}/°C.$$

TABLE 4-1

VOLUME DEPENDENCE ON SALT LEVEL IN THERMAL STORAGE TANKS AT 20°C

LEVEL (CM)	VOLUME (M**3)	LEVEL (CM)	VOLUME (M**3)
0.	0.000	230.	143.697
10.	1.495	240.	151.897
20.	4.316	250.	160.102
30.	8.066	260.	168.298
40.	12.390	270.	176.467
50.	16.935	280.	184.593
60.	21.654	290.	192.658
70.	27.052	300.	200.655
80.	32.822	310.	208.587
90.	38.919	320.	216.420
100.	45.300	330.	224.139
110.	51.923	340.	231.729
120.	58.742	350.	239.173
130.	65.715	360.	246.457
140.	72.943	370.	253.565
150.	80.334	380.	260.481
160.	87.883	390.	267.189
170.	95.570	400.	273.621
180.	103.381	410.	279.761
190.	111.298	420.	285.604
200.	119.305	430.	291.130
210.	127.385	440.	296.274
220.	135.521	450.	301.000

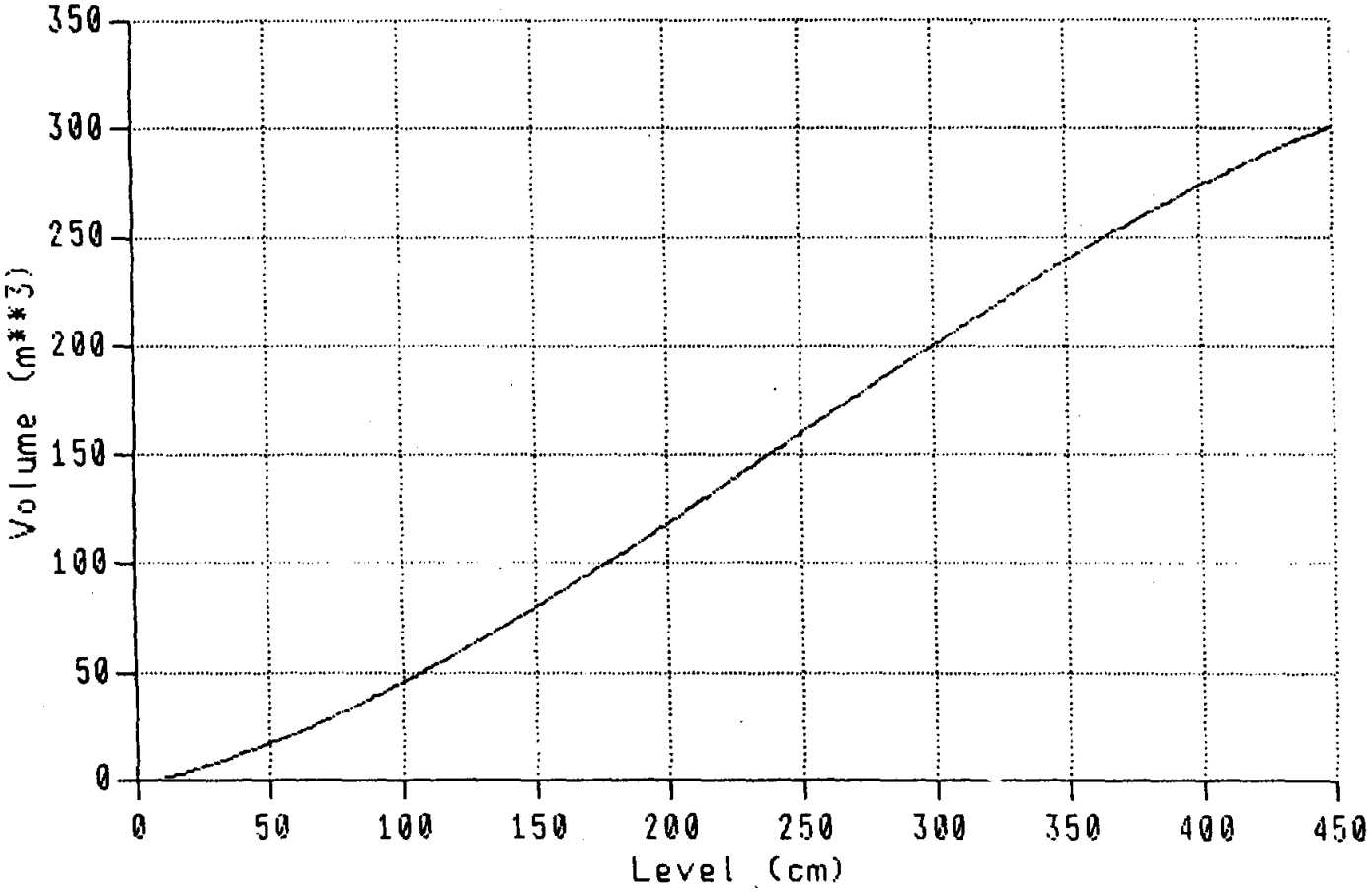

FIG 11 : VOLUME DEPENDENCE ON SALT LEVEL IN THERMAL STORAGE TANKS AT 20°C

5.0 TANK HEAT LOSS EVALUATION-EXPERIMENTS

The heat loss from the thermal storage tanks were derived from measurements of the cool-down rates dT dt deduced from four measuring campaigns: May 18.1984. Nov.16.1984. Jan.11.1985. and Feb.8.1985.

The main problem in measuring significant cool-down rates. is the very long time scale of the temperature decay because of the low tank heat loss. compared to the short time scale of salt temperature and volume variation during normal plant operation. During the four measuring campaigns. the salt level in the investigated tanks was kept constant and the only allowed energy flow was the tank heat loss.

5.1 EXPRESSION OF TANK HEAT LOSS

The heat loss of the bulk of salt in a tank is written :

$$P_s = -\frac{dU}{dt} = -\rho_s \cdot V_s \cdot C_{ps} \frac{dT}{dt} \qquad (1)$$

Similarly the expressions of the power lost by the metallic vessel and by the heat insulator read :

$$P_m = -M_m . C_{pm} \frac{dT_m}{dt} \qquad (2)$$

$$P_c = -M_c . C_{pc} dT_c/dt \qquad (3)$$

Where :

- ρ_s : average specific gravity of salt
- C_{ps}. C_{pm}. C_{pc} : Specific heat of salt. metal. insulation
- M_m. M_c : Total mass of metal. insulation.

Assuming an identical cooling rate of the salt. the vessel and the insulation. the total power loss of a tank reads :

$$P_L = -(\rho_s . V_s . C_{ps} + M_m . C_{pm} + M_c . C_{pc}) dT/dt \qquad (4)$$

5.2 EXPERIMENTAL DATA - TANK HEAT LOSS EVALUATION

Some examples of records from the tank cooling down experiments are given in Appendix of this report.

The cooling down rates measured during the four campaigns were used in expression (4) to evaluate the total heat loss of the investigated tanks. The heat losses of the vessel itself and of the insulation are derived from Equations (2) and (3).

The results of this analysis are presented in the following table :

TABLE 5-1 TANK HEAT LOSS EVALUATION

	Tank Ident.	Salt Volume m^3	Test duration (ms)	Cool-down rate (10^{-4}°C/s)	Initial salt temp. (°C)	Final salt temp. (°C)	Metal heat loss (kW)	Insulator loss (kW)	Salt heat loss (kW)	Total heat loss (kW)
First camp. May 18. 84	Cold Tank FKH001BA	263.2	4286	0.205	260	254.7	0.272	0.271	16.00	16.543
Sec. camp. Nov.16. 84	Cold Tank FKH001BA	140.65	1477	0.339	249	246	0.450	0.448	14.202	15.100
	Hot Tank FKH002BA	132.28	1477	0.678	328	322	0.899	0.898	26.00	27.800
Third camp. Jan.11. 85	Hot tank FKH002BA	7.26	1765	4.25	305	260	5.639	5.618	9.003	20.260
Fourth camp. Feb.8. 85	Hot Tank FKH002BA	297.5	4320	0.289	311	303.5	0.383	0.382	25.025	25.790

The results presented in Table 5-1 show that the vessel and the insulation have equivalent contributions to the total heat loss. These contributions are small (< 7 percent) in the cooling down experiments with large filling ratios.(> 40%).Obviously it was not the case on Jan.11.1985. the hot tank was almost empty. In this latter case. the heat loss of the salt was of the same order as that of the vessel and of the heat insulator.

The cool-down experiments described here start from initial temperatures appreciably lower than the design temperature of the hot tank (450°C). At the present date there is not yet available data at this temperature. In order to evaluate the heat loss of the hot tank at the design temperature. the data of Table 5-1 will be extrapolated as discussed in the next section.

6.0 TANK HEAT LOSS EVALUATION-ANALYTICAL DISCUSSION

In this section two regimes will be analysed :

a)The steady state regime ($\partial T / \partial t = 0$), when the salt temperature is kept constant.

b)The cooling down regime when the salt temperature is decreasing with time.

6.1 STEADY STATE REGIME

When the salt temperature is kept constant or when the cool-down of a thermal storage tank is very slow, because of the large amount of hot salt present, the steady state approximation ($\partial T / \partial t = 0$) can be used and a simple solution of the heat transfer equation in the insulation is derived. In addition, axial symmetry is assumed : $\partial T / \partial \theta = 0$. This is justified by the high thermal conductivity of the metal that does not allow large temperature gradients in the metallic vessel.

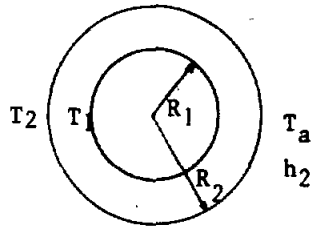

The heat propagation equation in the insulation then reads :

$$\nabla \cdot (\lambda(T) \nabla T) = 0$$

where $\lambda(T)$ = insulation thermal conductivity.

In cylindrical coordinates, we have :

$$\frac{1}{r} \cdot \frac{d}{dr}\left(r\lambda(T) \frac{dT}{dr}\right) = 0 \qquad (5)$$

The boundary conditions at R_1 and R_2 are :

at R_1, the heat flux φ_1 is : $\varphi_1 = -\lambda(T_1) \left.\frac{dT}{dr}\right|_{r=R_1}$

at R_2, the heat flux φ_2 is $\varphi_2 = h_2 \cdot (T_2 - T_a)$

Where h_2 is the heat transfer coefficient at the boundary R_2.

After integration Equation (5) becomes :

$$r\lambda(T)\frac{dT}{dr} = -\varphi_1 \cdot R_1 = -h_2(T_2 - T_a)R_2$$

An approximate solution of the above equation is obtained by integration assuming a constant averaged value of $\lambda(T)$:

$$T = T_1 - \frac{\varphi_1 R_1}{\lambda} \ln(r/R_1) \qquad (6)$$

With λ = average value of $\lambda(T)$

λ is a function of T_1 and T_2 and is given by the insulation manufacturer (Figure 12).

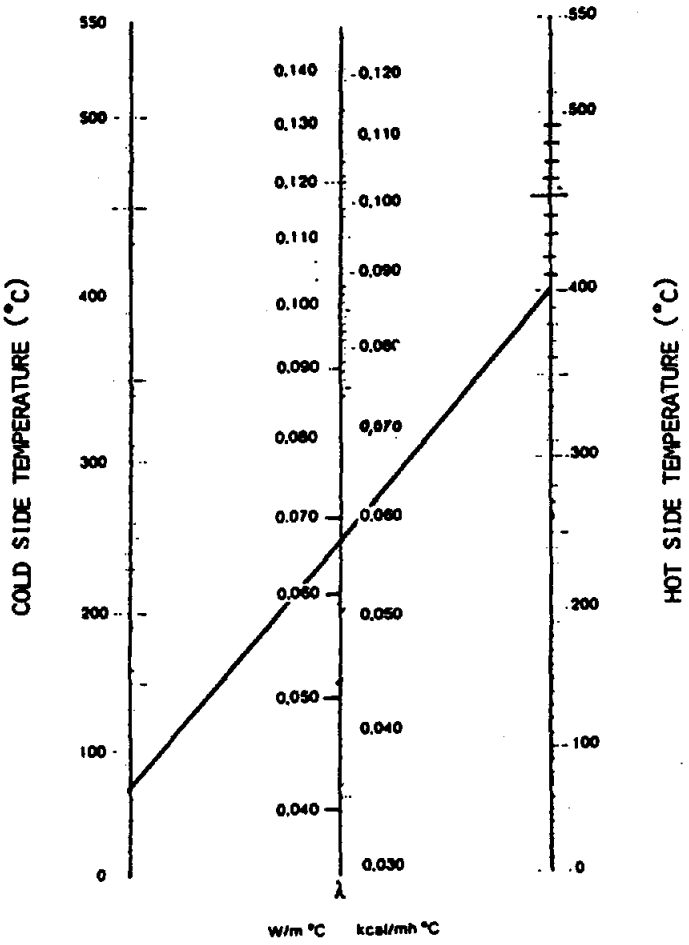

Example :

Hot side temperature : 400°C

Cold side temperature: 70°C

Thermal conductivity : 0.066 W/m°C

Characteristics :

Density : 110 kg/m^3

Specific heat : 837 J/kg°C

Maximum temperature : 600°C

FIG 12 : THERMAL CONDUCTIVITY CHART OF THE INSULATION

The boundary condition at $r = R_2$ is :

$$\varphi_1 . R_1 = \varphi_2 . R_2 = R_2 h_2 (T_2 - T_a) \qquad (7)$$

Eliminating the temperature T_2 from (6) and (7). the heat flux φ_2 is expressed :

$$\varphi_2 = h_2 (T_1 - T_a) / (1 + R_2 h_2 . \ln(R_2/R_1)/\lambda)$$

Multiplying φ_2 by the external area S_2 of the tank insulation. an analytical expression for the tank heat loss is obtained :

$$P_L = \varphi_2 S_2 = S_2 h_2 (T_1 - T_a)(1 + R_2 h_2 . \ln(R_2/R_1)/\lambda)^{-1} \qquad (8)$$

Using Equation (8) the heat loss has been evaluated with the conditions of the experiments described in Section 5 and the following parameters :

- External surface of insulation : $S_2 = 374\ m^2$
- Heat transfer coefficient at $r = R_2$: $h_2 = 10 W\ m^{-2}°C$
- Ambiant air temperature : $T_a = 20°C$
- $R_1 = 2.5m$. $R_2 = 2.9m$

TABLE 6-1

	Tank Ident.	Salt Temp. at R_1 T_1(°C)	Ext Temp. at R_2 T_2(°C)	Tank Heat Loss (theory) kW	Tank Heat Loss (measured) kW
1st camp.	Cold Tank FKH001BA	260	23	10.71	16.543
2nd camp.	Cold Tank FKH001BA	249	23	10.22	15.100
	Hot Tank FKH002BA	328	24.1	15.31	27.800
3rd camp.	Hot Tank FKH002BA	305	23.8	14.17	20.260
4th camp.	Hot Tank FKH002BA	311	23.90	14.47	25.790

It is seen in Table 6-1 that the total tank heat loss deduced by Equation (8) is appreciably smaller (< 65%) than the measured one. The discrepency between theory and experiment may be explained by the uncertainty on the insulation thermal conductivity. It is known that during the history of the plant, some salt leaks happened. It is possible that heat bridges, resulting from salt penetration into the insulation, might have formed, thus reducing the thermal resistance.

Experimental results are in better agreement with theory, assuming that the heat conductivity of the insulation has a linear temperature dependence :

$$\lambda = aT + b$$

Where the coefficients a and b can be evaluated by matching the heat losses with the experimental data :

We have :

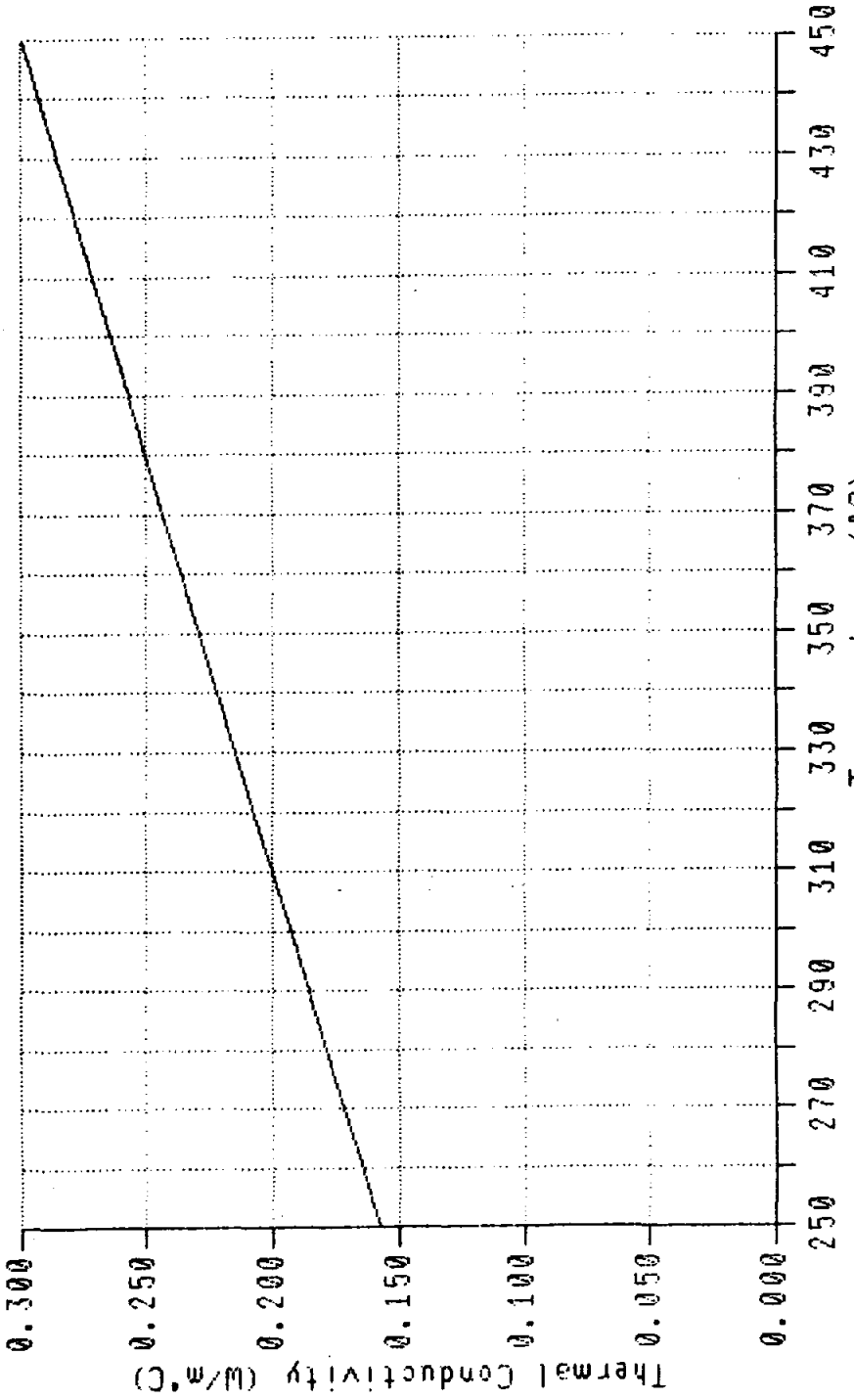

FIG 13 : ACTUAL THERMAL CONDUCTIVITY

$$r\lambda(T)dT/dr = -\varphi_1 R_1$$

Integrating the above equation, we obtain :

$$\int_{T_1}^{T_2}(aT + b)dT = -\varphi_1 R_1 \int_{R_1}^{R_2} dr/r$$

A second degree equation is thus derived for T_2 :

$$aT_2^2 + 2(b + h_2 R_2 \ln(R_2/R_1))T_2 - aT_1 - 2bT_1 - 2R_2 h_2 T_a \ln(R_2/R_1) = 0 \qquad (9)$$

Where T_1 and T_a are known.

As above, the tank heat losses can be written :

$$P_L = S_2 h_2 (T_2 - T_a) \qquad (10)$$

Using the values of P_L measured with $T_1 = 249°C$ and $T_1 = 328°C$, the two coefficients a and b are deduced from Equations (9) and (10).

$a = 7.1\ 10^{-4}$ W/m.°C.°C

$b = -0.02$ W/m.°C

The tank heat losses for any value of the temperature T_1 can now be evaluated, using the corresponding T_2 value given by Equation (9).

This method has been used to evaluate the tank heat loss at temperatures ranging from 250°C to 450°C. The results are listed in Table 6-2 and the heat loss temperaure dependence is plotted in Figure 14. It is seen that the tank heat loss at the design temperature of 450°C is $P_L = 55$ kW.

TABLE 6-2

TANK HEAT LOSS DEPENDENCE ON SALT TEMPERATURE

Temperature (°C)	Thermal conductivity (W/m°C)	Losses (kW)
250.0	0.1577	15.229
270.0	0.1719	16.097
290.0	0.1860	21.212
310.0	0.2002	24.558
330.0	0.2144	28.171
350.0	0.2286	32.015
370.0	0.2427	36.106
390.0	0.2569	40.443
410.0	0.2711	45.037
430.0	0.2853	49.868
450.0	0.2853	54.940

6.2 TANK COOL-DOWN MODEL

The cool-down rates measured in the experiments described in Section 5 can be estimated by a simple model based on the electrical analogy of the cool- down process with a resistor capacity discharge.

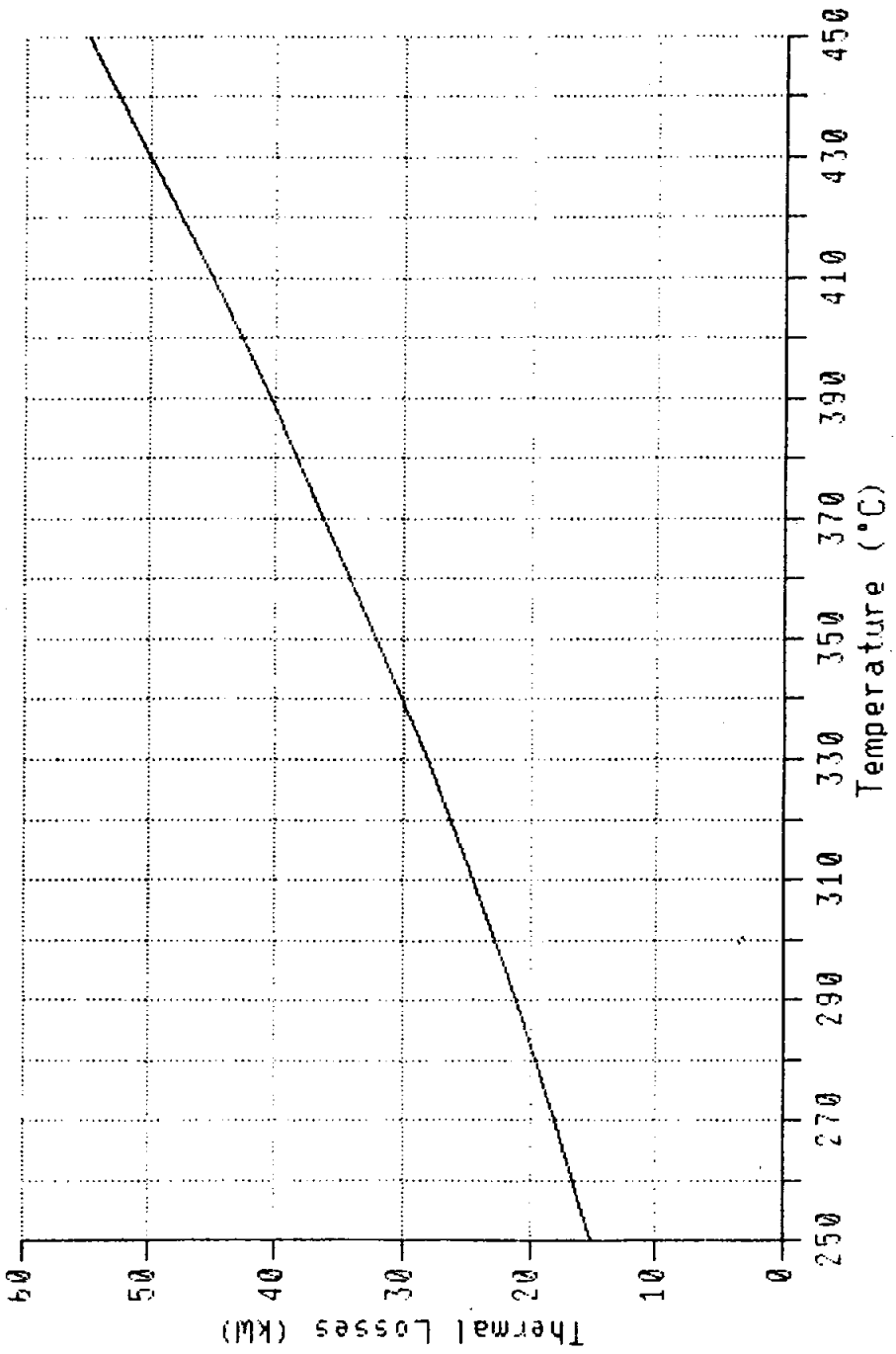

FIG 14 : TANK HEAT LOSS DEPENDENCE UPON SALT TEMPERATURE

6.2.1 TANK COOL-DOWN EQUATION

Let the tank initial temperature be Ti and the thermal resistance be R. The tank temperature time dependence is expressed by :

$$T = Ta + (Ti-Ta)Exp(-t/RC) \qquad (11)$$

where :

$$C = \rho sVsCps + MmCpm + McCpc$$

The thermal resistance R is obtained from the cooling down measurements by the relation:

$$R = \frac{t}{C}\left[\ln \frac{T_i - T_a}{T - T_a}\right]^{-1} \qquad (12)$$

The total heat loss from the tank then reads :

$$P_L = (T - T_a)/R \qquad (13)$$

6.2.2 TANK THERMAL RESISTANCE AND HEAT LOSS ESTIMATION

The data from the cool-down experiments are used to evaluate the thermal resistance R (Eq.12) and the heat loss (Eq.13) of both tanks. The results obtained by this method are listed in Table 6-3. The assumed ambiant temperature is Ta = 20°C.

TABLE 6-3

Tank Ident.	t (mn)	Ti (°C)	T (°C)	C (MJ/°C)	R (°C/W)	Tank Heat Loss (kW)
Cold Tank FKH001BA	4286	260	254.7	804.83	0.01431	16.406
Cold Tank FKH001BA	1477	249	246	417.50	0.01609	14.046
Hot Tank FKH002BA	1477	328	322	410.37	0.01100	27.455
Hot Tank FKH002BA	1765	305	260	47.75	0.01288	18.634
Hot Tank FKH002BA	1765	311	303.5	889.37	0.01116	25.403

Comparison of Tables 6-3 and 5-1 shows that the heat loss derived from the experimental results by Equations (4) and (13) have very close values.

From the experimental results, the average value of the tank thermal resistance is :

Rmc = 0.0152°C/W for the cold tank,

Rmh = 0.0117°C/W for the hot tank.

For some specific applications, for instance, the use of the SOLTES code, the parameter used is R^{-1}. We obtain :

R^{-1}mc = 65.8 W/°C for the cold tank,

R^{-1}mh = 85.5 W/°C for the hot tank.

The external surface of both tanks is 297 m^2.The derived heat transfer coefficients thus are :

0.2290W/m^2°C for the cold tank.

and 0.2889W/m^2°C for the hot tank.

Tank power loss dependence upon T_a

The variation of the power loss from a tank for a variation ΔTa of the ambiant temperature Ta, can be derived from Equation (13) as follows :

$$|\Delta P_L|/P_L = |\Delta T_a|/(T - T_a)$$

therefore :

$$|\Delta P_L|/P_L < |\Delta T_a|/(T - T_a)$$

For the cold tank, the initial temperature is typically Ti = 250°C. A variation ΔTa of 10°C would be responsible of a 4% variation of P_L.

Similarly considering now the hot tank, with an initial temperature Ti = 300°C, a Ta variation of 10°C would result in a 3.5% variation of P_L.

6.2.3 COMPARISON OF EXPERIMENTAL RESULTS WITH DESIGN

Cool-down predictions of the hot tank for an initial temperature Ti = 425°C and various salt volumes, were computed by the manufacturer. The resulting temperature decay curves are available in Ref. 2 . Taking R = Rmh, an initial temperature Ti = 425°C, the tank temperature derived by Equation (11) for a 100 hours cooling are listed in Table 6-4 for several salt volumes in the hot tank. For comparison the corresponding temperatures predicted by the manufacturer are listed in the same table.

TABLE 6-4

COMPARISON OF SALT TEMPERATURE AFTER 100 HOURS COOL-DOWN.

EXPERIMENTAL RESULTS MANUFACTURER PREDICTIONS

Filling Ratio %	Salt Weight (x10^{3}kg)	C(MJ/°C)	T(°C) Experiment + Cooling Model	T(°C) Manufacturer (DSE)
3	13.86	46.968	230.	220
5	23.10	61.954	266.5	257
10	46.2	99.418	317.	327
15	69.3	136.882	343.5	354
20	92.4	174.346	359.5	369
30	138.6	249.274	378.	389
40	184.8	324.202	388.4	399
50	231	399.130	395.	406
60	277.2	474.058	399.5	410
75	346.5	586.450	404.3	415

From Table 6-4 it can be observed that our cool-down model using the experimental value of Rmh is in reasonable agreement (ΔT/T < 5%) with the manufacturer predictions. The maximum discrepancy (ΔT/T = 5%) is observed in the case of small salt filling ratios(< 10%), when the cool-down rate is faster and the temperature uncertainty is larger.

6.2.4 SALT TEMPERATURE HOMOGENEITY

There is no direct measurement of the salt temperature distribution in the thermal storage tanks. However, there is indirect evidence of the existence of temperature gradients possibly associated with some stratification. Indeed the thermocouples measuring the outside metal temperature of the tanks indicate spatial temperature distribution that can be interpreted in terms of salt stratification.

a) Measuring campaign of Nov.16,1984.

The existence of a temperature gradient is shown by the experimental data presented in Table 6-5 (measuring campaign of Nov.16,1984). The measuring cross sections and the thermocouple reference are shown in Figures 9 and 10.

TABLE 6-5

METAL TEMPERATURE DISTRIBUTION DURING THE MEASURING CAMPAIGN OF NOV.16,1984

The position of cross sections and thermocouples is shown in Fig.9 and 10.

Measuring Cross Section Tank	**C1 Thermocouple, T(0)→T(t)**	**C2 Thermocouple, T(0)→T(t)**	**C3 Thermocouple, T(0)→T(t)**
Hot Tank (Salt level: 2.17m)	5MT,298→292 4MT,321.5→316 6MT,322→316	13MT,317.→309 12MT,321.→315 14MT,321.5→315	21MT,306→300 20MT,317.6→311.2 22MT,320→314
Measuring Cross Section Tank	**T1 Thermocouple, T(0)→T(t)**	**T2 Thermocouple, T(0)→T(t)**	**T3 Thermocouple, T(0)→T(t)**
Cold Tank (Salt level: 2.26m)	29MT,235.6→232 28MT,239.2→235.6 30MT,241.2→237.2	37MT,240→236.4 36MT,243.6→240 38MT,245.2→241.6	45MT,240.8→237.2 44MT,244.8→241.2 46MT,246→243.2

In the hot tank cross section C_1, (the section where the pumps are located), a temperature difference of about 20°C is observed between the bottom value (5MT) and the value at h = 0.73m where 4 MT and 6 MT are located. Similarly in cross section C_3, a temperature difference of 12°C is observed between 21 MT and 20 MT or 22 MT. A similar, but smaller temperature difference is observed in cross section C_2.

There are several possible interpretations of the temperature gradients observed in the cross sections C_1, C_2, and C_3

These temperature gradients can be interpreted as due to the influence of heat bridges associated with the tank supports. Another possibility is that they might result from some stratification occuring in the salt. Also combination of these two effects is very plausible.

A similar situation, with lower temperature gradient, is observed in the cold tank as shown by the temperature measurements in the cross sections T_1,T_2 and T_3 in Table 6-5.

7.0 ANALYSIS OF TYPICAL DAY OF THERMAL STORAGE OPERATION

In this section the energy stored in both storage tanks will be evaluated and its evolution will be analyzed over a typical day of plant operation.

The energy stored in the salt will be taken positive when the salt temperature is higher than the reference value of 250°C.

There are two possible methods for evaluating the thermal energy stored in a salt tank. One of them consists in measuring the salt level and then deducing the salt volume in the tank. Knowing the salt volume and the salt temperature, the stored energy is immediately obtained. The other method is based on the energy flow measurements at the inlet and the outlet of the tank.

Figure 8 shows the location of the measuring sensors used for this evaluation.

7.1 THE SALT LEVEL METHOD

The salt level is measured approximately every minute and the salt volume is deduced as described in Section 4. The thermal energy stored in the tank is then evaluated by the expression :

$$E(t) = M_s(t).C_{ps}(T_s(t) - 250)/3.6x10^9 \qquad (14)$$

Where :

- E(t): Stored energy in MWh,
- Ms(t): Salt mass in the tank in kg,
- Cps : Specific heat of Hitec (1.561 kJ/kg°C)
- Ts: Average salt temperature in the tank (°C).

The salt mass is derived from the salt volume. The salt volume itself is derived from the salt level measurements. The probes used for the salt level measurements are the bubble probes :

- FKH001MN and FKH003MN in the cold tank,
- FKH002MN and FKH004MN in the hot tank.

There are several ways to evaluate the salt temperature in the considered tank. A possible method is to use the metal temperature measured by the thermocouples placed on the thermal storage tank. The other method is to use the measured salt temperature at the outlet of the thermal storage tank. In the following analysis the latter method will be used.

7.2 THE INLET/OUTLET SALT FLOW METHOD

The energy balance of each storage tank can be expressed in terms of the inlet and outlet salt flow and of the heat loss.

Cold tank energy balance

The cold tank energy balance is written :

$$E_c(t) = C_{ps}\int_{t_o}^{t}\left[Q_{INC}(\tau)(T_{INC}(\tau) - 250) + Q_{RECY}(\tau)(T_{RECY}(\tau)-250) - Q_{OUT}(\tau)(T_{OUT}(\tau)-250)\right]d\tau$$
$$-\int_{t_o}^{t}P_{LC}(\tau)d\tau - \int_{t_o}^{t}P_{LDC}(\tau)(1 - F)d\tau - \int_{t_o}^{t}P_{LCP}(\tau)d\tau + E_c(t_o) \qquad (15)$$

Where :

- $Q_{INC}(t)$: Inlet salt flow into the cold tank , measured by the flowmeter FKH001MD.
- $Q_{RECY}(t)$: Recycling salt flow measured by FRS002MD when the three way-valve FRS009VS is in Position 0.
- $Q_{OUTC}(t)$: Outlet salt flow from the cold tank measured by the flowmeter FRS002MD.
- $T_{INC}(t).T_{RECY}(t).T_{OUTC}(t)$: Inlet, Recycling and Outlet salt temperatures.
- $P_{LC}(t)$: Cold tank heat loss.
- $P_{LDC}(t)(1-F)$: Downcomer heat loss while on the recycling mode.(F = 1 when FRS009VS is connecting with the hot tank. F = 0 when connecting with the cold tank).
- P_{LCP}: Cold pipe heat loss. The cold pipe considered here is the pipe connecting the steam generator outlet with the cold tank inlet.
- $E_c(t_o)$: Energy stored in the cold tank at t_o

In Equation (15) the temperatures $T_{INC}(t)$, $T_{RECY}(t)$, and $T_{OUTC}(t)$ are measured at Positions A, D,C respectively in Figure 8. For this reason the heat loss of the downcomer and of the pipe connecting the steam generator with the cold tank inlet must be taken into account and are expressed by the 4th and the 5th terms on the right side of Equation 15.

Hot tank energy balance

Similarly the hot tank energy balance is written :

$$E_H(t) = C_{ps}\int_{t_o}^{t}\left[Q_{INH}(\tau)(T_{INH}(\tau) - 250) - Q_{OUTH}(\tau)(T_{OUTH}(\tau) - 250)\right]d\tau$$
$$-\int_{t_o}^{t}P_{LH}(\tau)d\tau - \int_{t_o}^{t}P_{LDC}(\tau)F\,d\tau - \int_{t_o}^{t}P_{LHP}(\tau)d\tau + E_H(t_o) \qquad (16)$$

Where :

- $Q_{INH}(t)$, $Q_{OUTH}(t)$: Hot tank Inlet, Outlet salt flow.
- $T_{INH}(t)$, $T_{OUTH}(t)$. Hot tank Inlet, Outlet salt temperatures measured at positions D and B respectively in Figure 8.
- $P_{LH}(t)$: Hot tank heat loss.
- $P_{LDC}F$: Downcomer heat loss when FRS009VS is connecting with the hot tank.
- $P_{LHP}(t)$: Hot pipe heat loss. The hot pipe considered here is the pipe connecting the hot tank outlet with the steam generator inlet.
- $E_H(t_o)$: Energy stored in the hot tank at the initial time t_o.

7.3 EXPERIMENTAL RESULTS

Measurements recorded on March 6, 1985 are presented in Figures 15 to 26.

Figure 15 shows the incoming solar power and the receiver power output.

Figure 16 represents the receiver energy output obtained by integration of the previous result. The total direct solar incoming energy on the heliostat field during this day was 71.287 MWh. The receiver total energy output during the same period was 43.13 MWh. leading to a daily heliostat-receiver average efficiency of 0.605. The plant was connected to the grid from 8h30'to 12h42'and delivered 7.054 MWhe (gross production).

Figure 17 shows the receiver outlet temperature variation. The lower curve in this figure is a signal indicating when the three-way valve FRS009VS is connected with the hot tank or with the cold tank.

Figures 18 to 20 show the steam generator behaviour. On Figure 18 the inlet and the outlet salt temperature variation show the plateau and seven peaks corresponding to the flow of salt in the steam generator. When there is no salt flow, the temperatures are seen to decay.

Figure 19 shows the power transferred from the salt to the steam generator. The plateau from 8h30'to 12h42'indicated the heat power transferred for electricity production and the seven remaining peaks represent the heat power transferred for preheating or keeping hot the steam generator and the steam loop. In Figure 20. the energy transferred from the salt to the steam generator is represented.It is seen that the total energy transferred to the steam generator is 34.57 MWh. This energy can be broken down in two components: the heat converted into electricity 31.6 MWh. and the heat used for preheating and keeping hot the steam generator and the steam loop 2.97 MWh.

Figures 21 to 26 illustrate the behaviour of the thermal storage subsystem itself.

Figure 21 shows the salt volume variation in both storage tanks. It is seen that the salt volume in the hot tank is constant from 0 to 7h10' because no salt is sent to the steam generator. From 7h10' to 8h30' the salt level decrease is due to the salt flow peaks for preheating the steam generator and the steam loop. From 8h30' to 12h42', the salt level in the hot tank decreases progressively because the receiver output is smaller than the steam generator input during the electricity production phase. From 12h42'to 16h.the salt level rises again because the receiver salt output is sent to the hot tank. After 17h the receiver is shutdown. and no more salt is sent to the hot tank. The salt level remains almost constant with only some small amplitude steps correlated with the salt flow peaks sent to the steam generator. There are two kinds of ripples on the hot tank salt level trace. The first kind of ripples is correlated with the salt flow pulses to the steam generator. The second kind is correlated with the direction change of the three-way valve FRS009VS.as indicated in Figure 17.

The salt level in the cold tank varies obviously in the opposite way to the one in the hot tank. This behaviour is normal because the total amount of salt must remain constant.

Figure 22 shows the heat power transferred to the hot tank. This power is the sum of two leading terms : The receiver power output which gives a positive contribution when the valve FRS009VS is connecting with the hot tank and the steam generator heat power input which gives a negative contribution. The sum of these two contributions explains clearly the shape of the observed trace.

Figure 23 represents the heat power transferred to the cold tank. The positive contributions are mostly due to the receiver salt output when the valve FRS009VS is connecting with the cold tank in the recycling mode. The negative contributions are mainly due either to the salt volume decrease in the tank or to the input of cold salt at a temperature lower than 250°C coming from the steam generator.

Figure 24 shows the variation of the stored energy in the hot tank (upper trace) and in the cold tank (lower trace).

Figure 25 shows the stored energy variation in both tanks computed by the salt flow rate method.

The comparison of Figures 24 and 25 shows that the traces representing the stored energy in the hot tank are in good agreement.

Nevertheless some deviation can be observed on the traces representing the stored energy in the cold tank. There are two possible explanation of this fact : the first one is fundamental. The salt level method gives directly the stored energy in the tank whereas the salt flow method gives, in addition, the contributions of the tank and piping heat losses, as shown by Equations (15) and (16). These losses should be evaluated independently and corrections should be brought to the results shown in Figure 25. The second possible reason for the observed discrepancy is the uncertainty of the measurements: the salt flow measurement has an uncertainty of 4 to 5 percent. In addition, the salt temperature in a tank is difficult to define precisely because of the temperature gradients which might be responsible for a few degrees Celsius deviation from the measured temperature.

Finally Figure 26 represents the variation of the total energy stored in the whole thermal storage subsystem (including both tanks). This result is derived by the salt level method. It is seen that at the initial time t_o = 0h the total stored energy is 23.73 MWh, at 12h42' there is a minimum with a stored energy of 7.24 MWh, the stored energy then rises to a maximum value of 36.6 MWh at 17h and finally shows a plateau of 29.55 MWh at 24h. The thermal storage energy balance will be discussed in the next section.

7.4 THERMAL STORAGE ENERGY BALANCE

The thermal storage subsystem energy balance over a period of time (t_o,t) can be expressed by adding Equations (15) and (16) of the previous section. This leads to the following expression:

$$E(t) - E(t_o) = E_{SR}(t_o,t) - W_{DC}(t_o,t) - E_{SG}(t_o,t) - W_{SGP}(t_o,t) - W_{TS}(t_o,t) \quad (17)$$

Where :

- E(t) is the total energy stored in the hot tank and in the cold tank as shown in Figure 23:
  $$E(t) = E_H(t) + E_C(t)$$
- $E(t_o)$ is the initial value of E(t) at time t_o
- $E_{SR}(t_o,t)$ is the energy output of the solar receiver. This energy is measured by difference of the energy flow in D and in C of the receiver loop (Figure 8). It can be seen that :

$$E_{SR}(t_o,t) = C_{ps}\int_{t_o}^{t}\left[Q_{INH}(\tau)\,(T_{INH}(\tau)-250) + Q_{RECY}(\tau)\,(T_{RECY}(\tau)-250) - Q_{OUTH}(\tau)\,(T_{OUTH}(\tau)-250)\right]d\tau$$

- $W_{DC}(t_o,t)$ is the downcomer heat loss, which gathered two terms in Equations (15) and (16):

$$W_{DC}(t_o,t) = \int_{t_o}^{t} P_{LDC}(\tau)F\,d\tau + \int_{t_o}^{t} P_{LDC}(\tau)(1-F)\,d\tau$$

- $E_{SG}(t_o,t)$ is the salt heat delivered to the steam generator. This quantity is directly measurable, by combining the salt flow measured by FRS001MD and the steam generator inlet and outlet salt temperatures measured in B and A.
- $W_{SGP}(t_o,t)$ is the heat loss of the steam generator piping, i.e. of the hot pipe and of the cold pipe connecting the steam generator with the hot tank and with the cold tank. This heat loss is expressed by :

$$W_{SGP}(t_o,t) = \int_{t_o}^{t} P_{LCP}(\tau)\,d\tau + \int_{t_o}^{t} P_{LHP}(\tau)\,d\tau$$

There is no available direct measurement of this quantity.

- $W_{TS}(t_o,t)$ is the total heat loss of the thermal storage tanks :

$$W_{TS}(t_o, t) = \int_{t_o}^{t} P_{lC}(\tau)d\tau + \int_{t_o}^{t} P_{lH}(\tau)d\tau$$

This quantity is known according to the heat loss measurements described in Sections 5 and 6.

In order to validate the above evaluation of the thermal storage subsystem energy balance, the different terms of Equations (17) are now estimated on the basis of the experimental data of March 6, 1985. The results are presented in Table 7-1.

The results listed in the upper part of Table 7-1 show that the energy balance of the thermal storage subsystem is satisfactorily understood within the uncertainty of the measurements.

Nevertheless, this uncertainty is too large to allow a significant evaluation of the heat loss total by using the expression :

$$\text{Heat loss total} = E_{SR}(0,t) - E_{SG}(0,t) + E(0) - E(t)$$

Indeed the error on each term of this equation is of the same order as the heat loss total. Therefore, this heat loss is evaluated separately in the lower part of Table 7-1, by using independent measurements or calculations.

TABLE 7-1

THERMAL STORAGE SUBSYSTEM ENERGY BALANCE AFTER MARCH 6, 85
EXPERIMENTAL DATA

Energy Term	Symbol	$t_o = 0h$	$t_1 = 24h$
Stored energy in the cold tank	$E_c(t)$	1.	0.84
Stored energy in the hot tank	$E_H(t)$	22.73	28.71
Total stored energy	$E(t)$	23.73	29.55
Receiver output (measured between C and D in Figure 8)	$E_{SR}(0,t)$	0.	43.13
Heat transferred to the steam generator	$E_{SG}(0,t)$	0.	34.57
Heat loss total(based on measurements) $E_{SR}(0,t)-E_{SG}(0,t)-E(0)-E(t)$	$W_{DC}(0,t) + W_{SGP}(t_o,t) - W_{TS}(0,t)$	0.	2.74
Heat loss evaluation			
Hot tank 400°C (43kW)	$W_{LH}(0,t)$	0.	1.032
Cold tank 250°C (15.2kW)	$W_C(0,t)$	0.	0.365
Heat storage subsystem total	$W_{TS}(0,t)$	0.	1.397
Downcomer 250°C (20 kW)		0.	0.230
400°C (34kW)		0.	0.430
Downcomer total	$W_{DC}(0,t)$	0.	0.660
Steam generator piping			
Hot pipe 400°C (3kW)		0.	0.038
Hot pipe 250°C (1,2kW)		0.	0.012
Cold pipe 250°C (0.817kW)		0.	0.020
Steam Generator piping total	$W_{SGP}(0,t)$	0.	0.070
Heat loss total(evaluated)	$W_{TS}(0,t) + W_{DC}(0,t) + W_{SGP(0,t)}$	0.	2.127

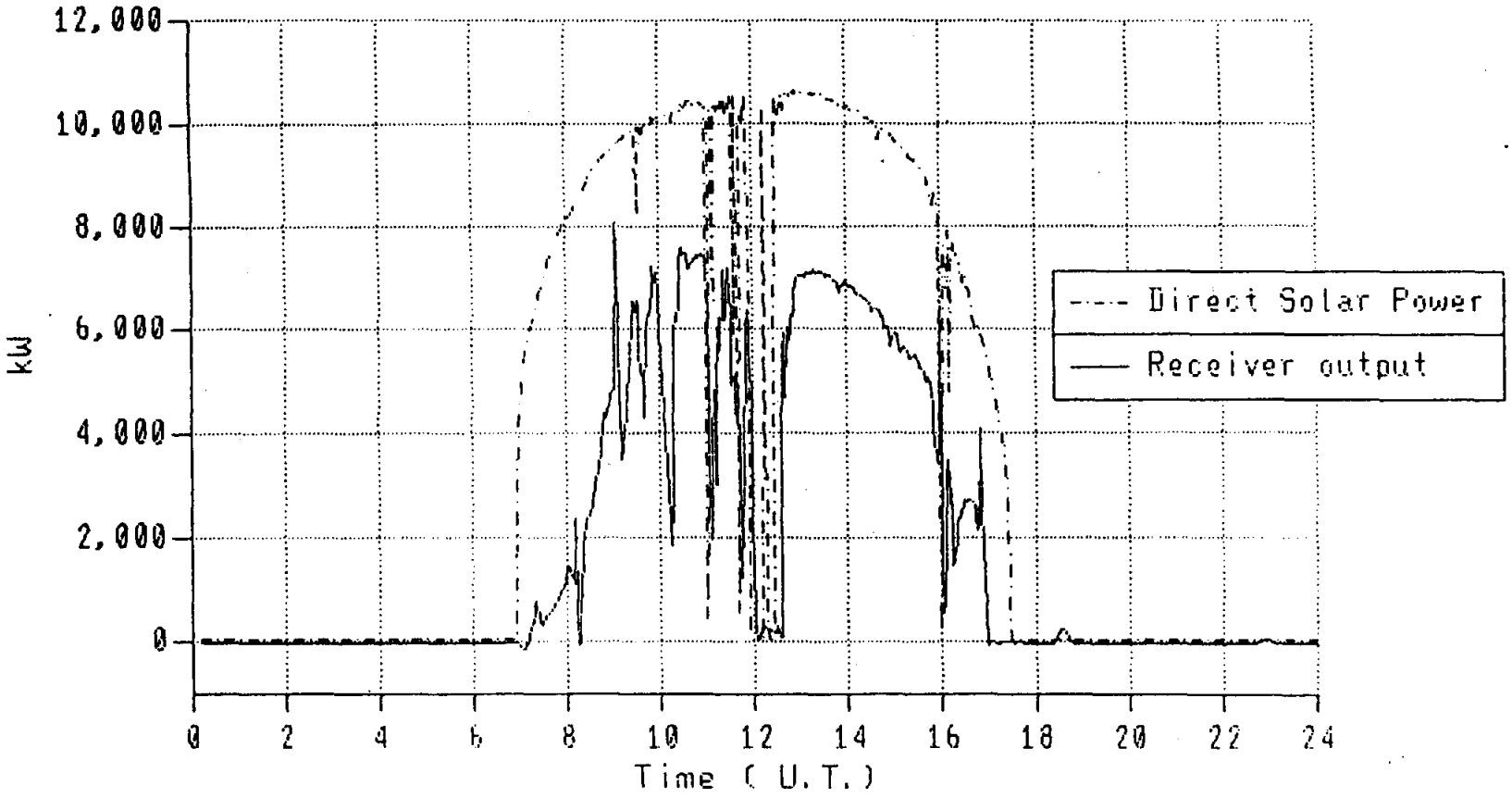

FIG 15: THEMIS, MARCH 6, 1985 . INCOMING DIRECT SOLAR POWER AND RECEIVER SUBSYSTEM OUTPUT

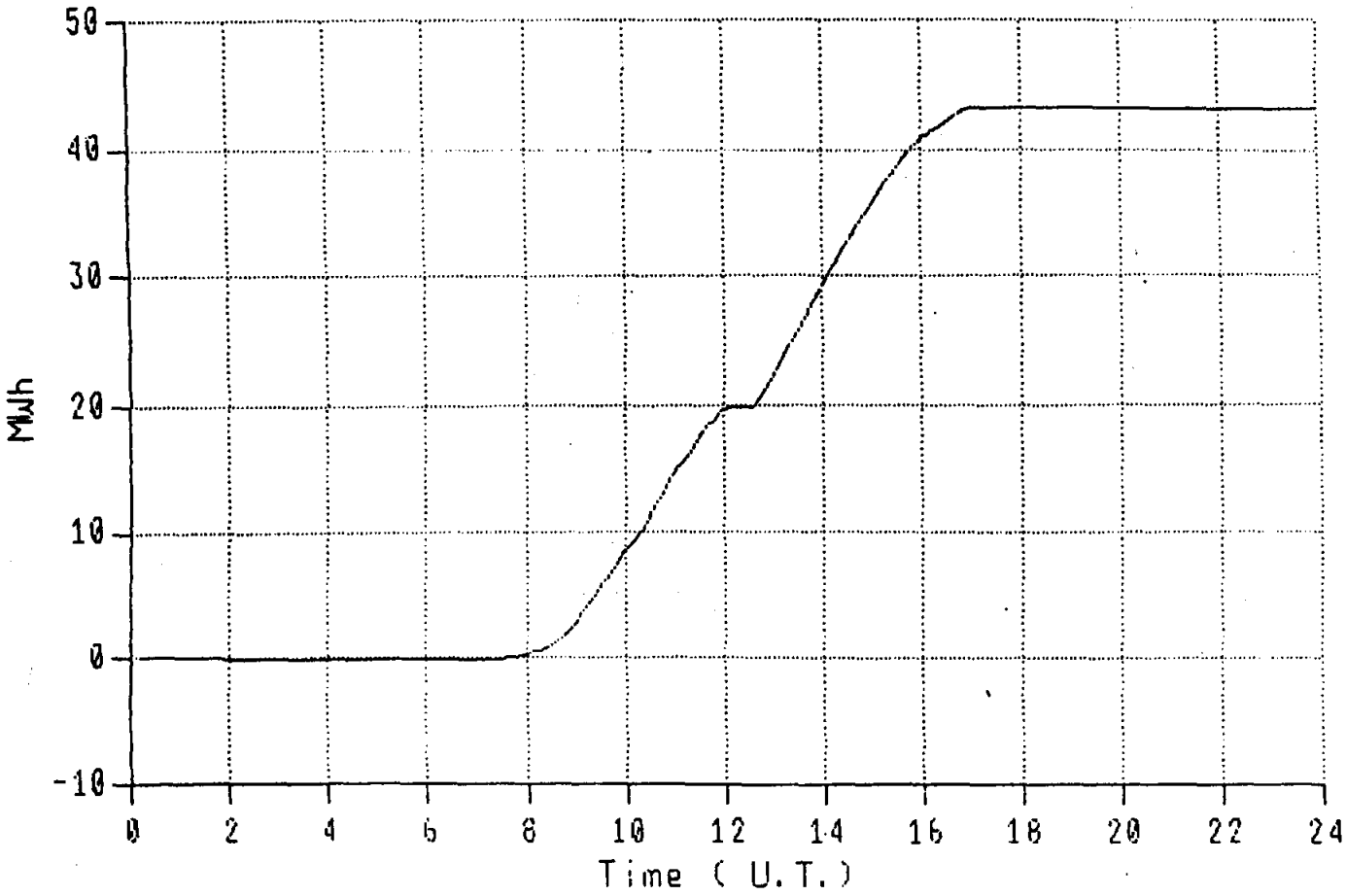

FIG 16 : THEMIS, MARCH 6, 1985 , RECEIVER SUBSYSTEM ENERGY OUTPUT

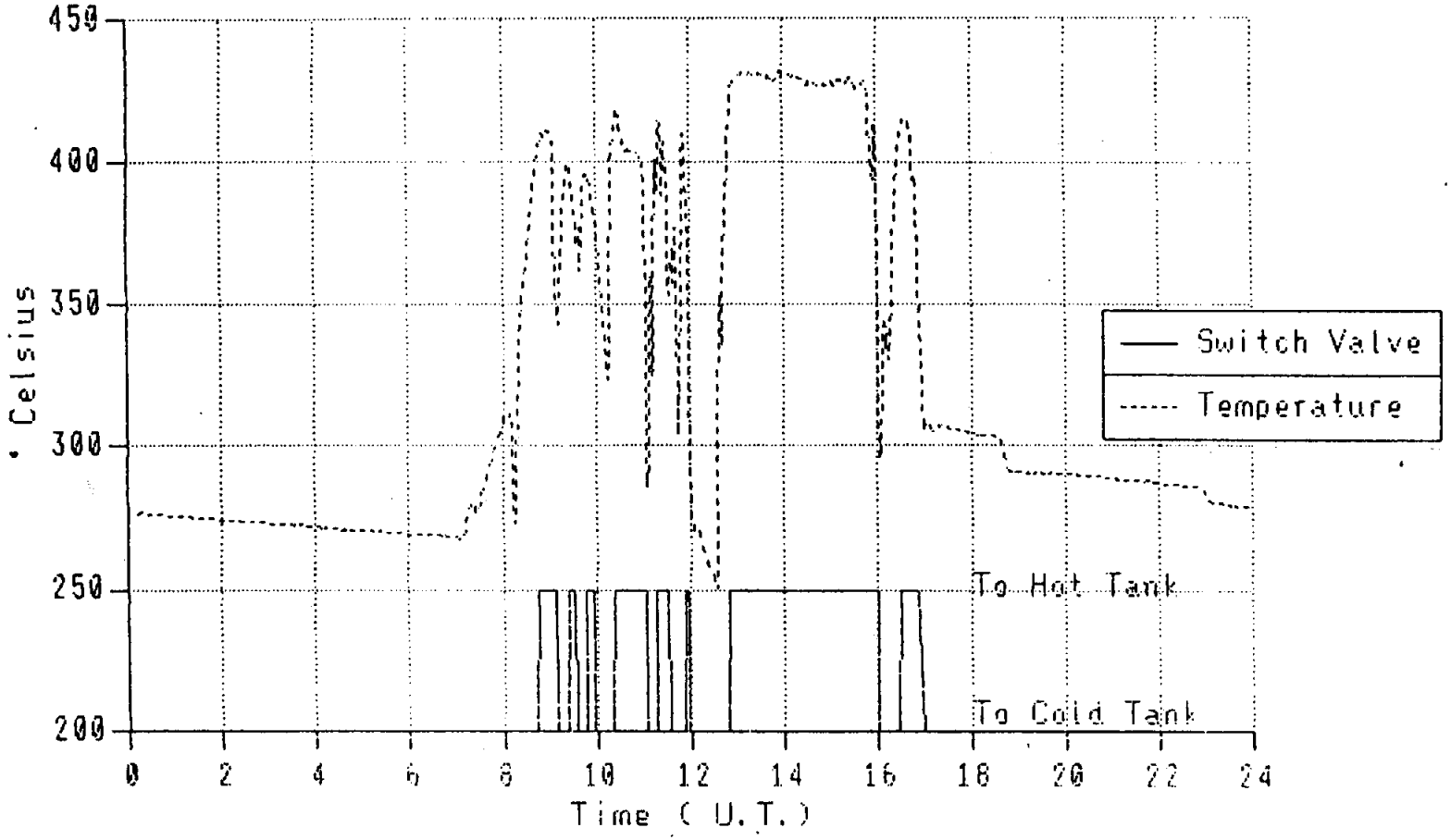

FIG 17 : THEMIS, MARCH 6, 1985 , BUFFER TANK OUTLET TEMPERATURE

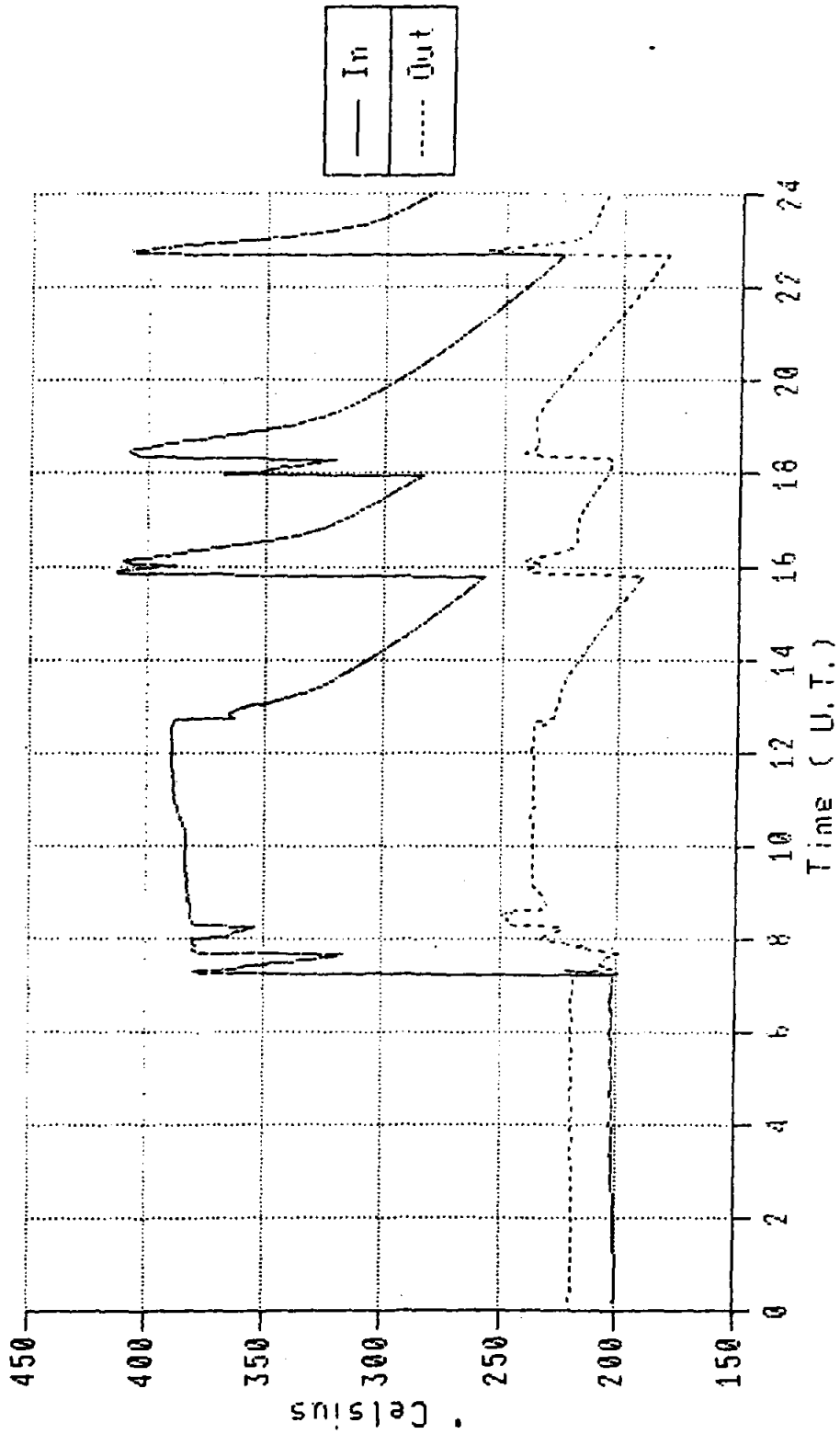

FIG 18 : THEMIS, MARCH 6, 1985 . STEAM GENERATOR INLET AND OUTLET TEMPERATURE

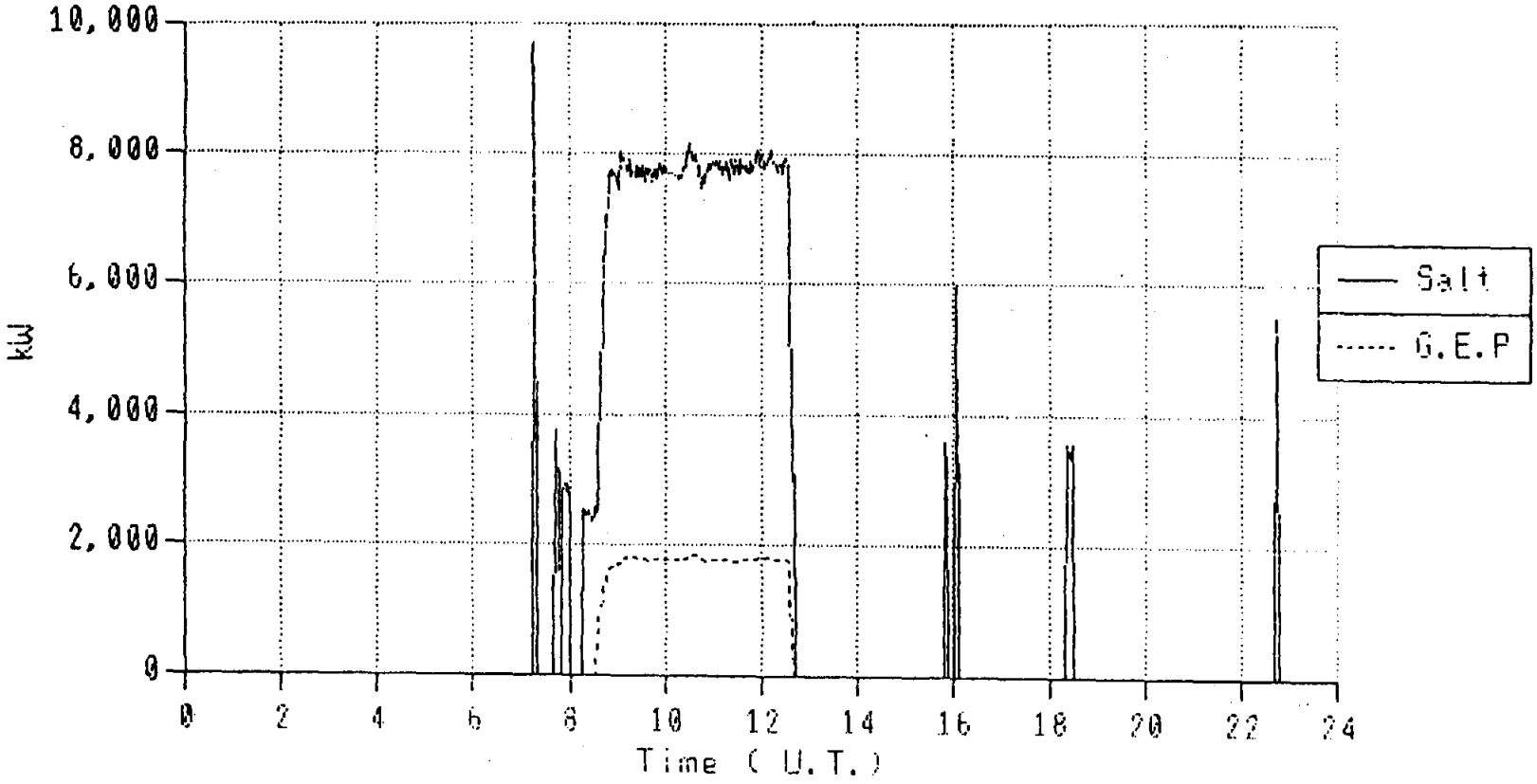

FIG 19 : THEMIS, MARCH 6, 1985 . HEAT TRANSFERRED FROM THE SALT TO THE STEAM GENERATOR, AND GROSS ELECTRICITY PRODUCTION

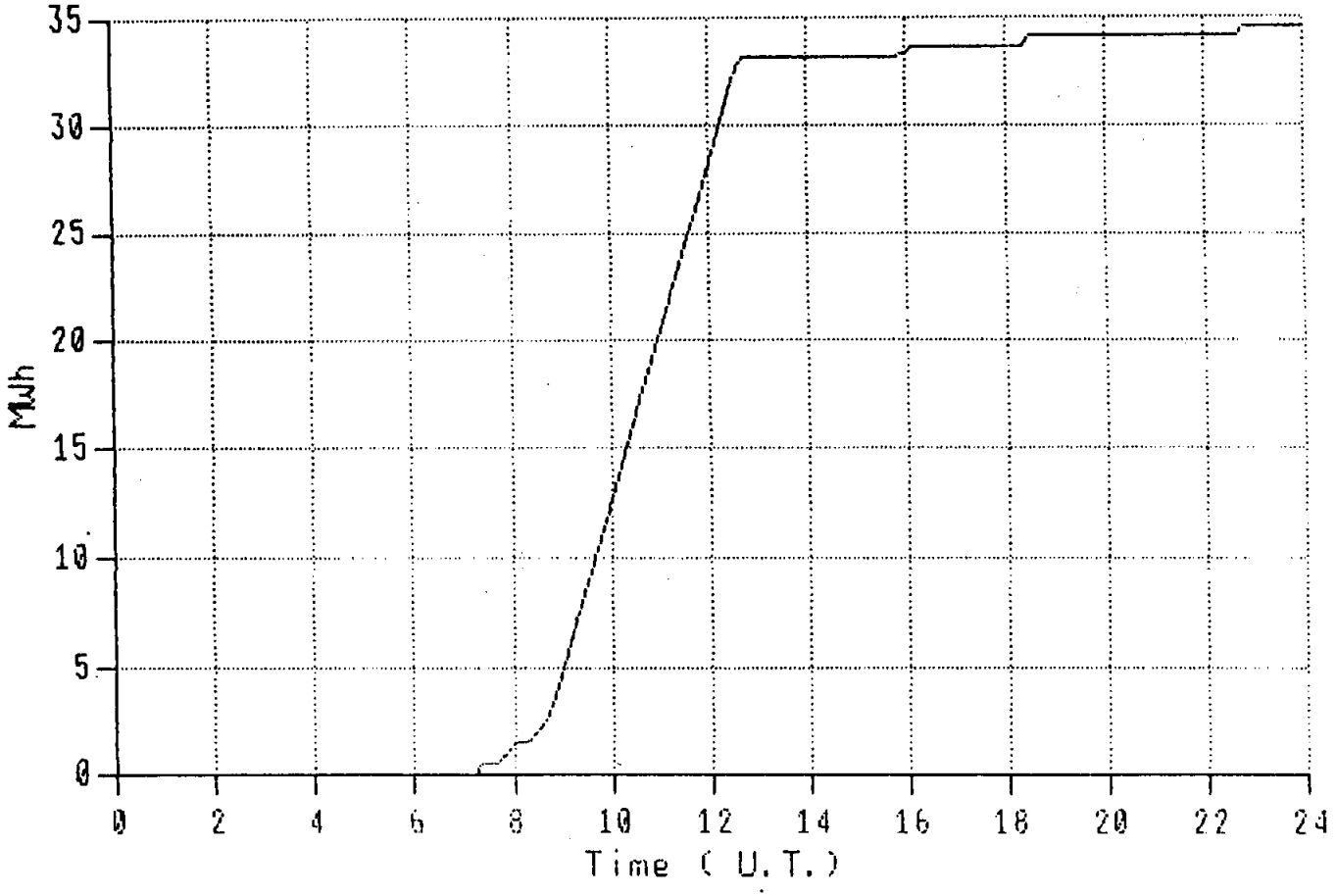

FIG 20 : THEMIS, MARCH 6, 1985 . ENERGY TRANSFERRED FROM THE SALT TO THE STEAM GENERATOR

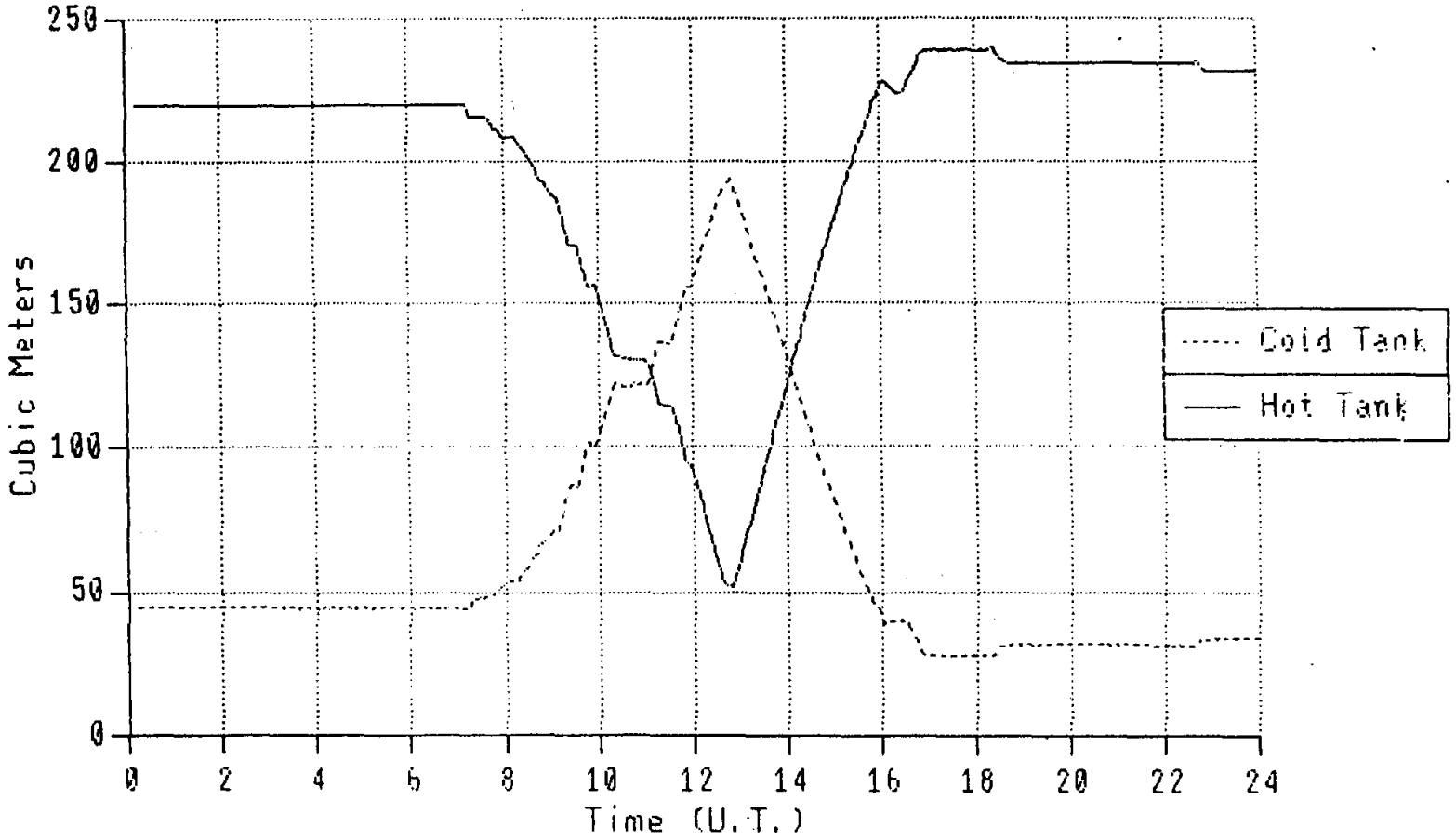

FIG 21 : THEMIS, MARCH 6, 1985 . SALT VOLUME VARIATION IN THE STORAGE TANKS

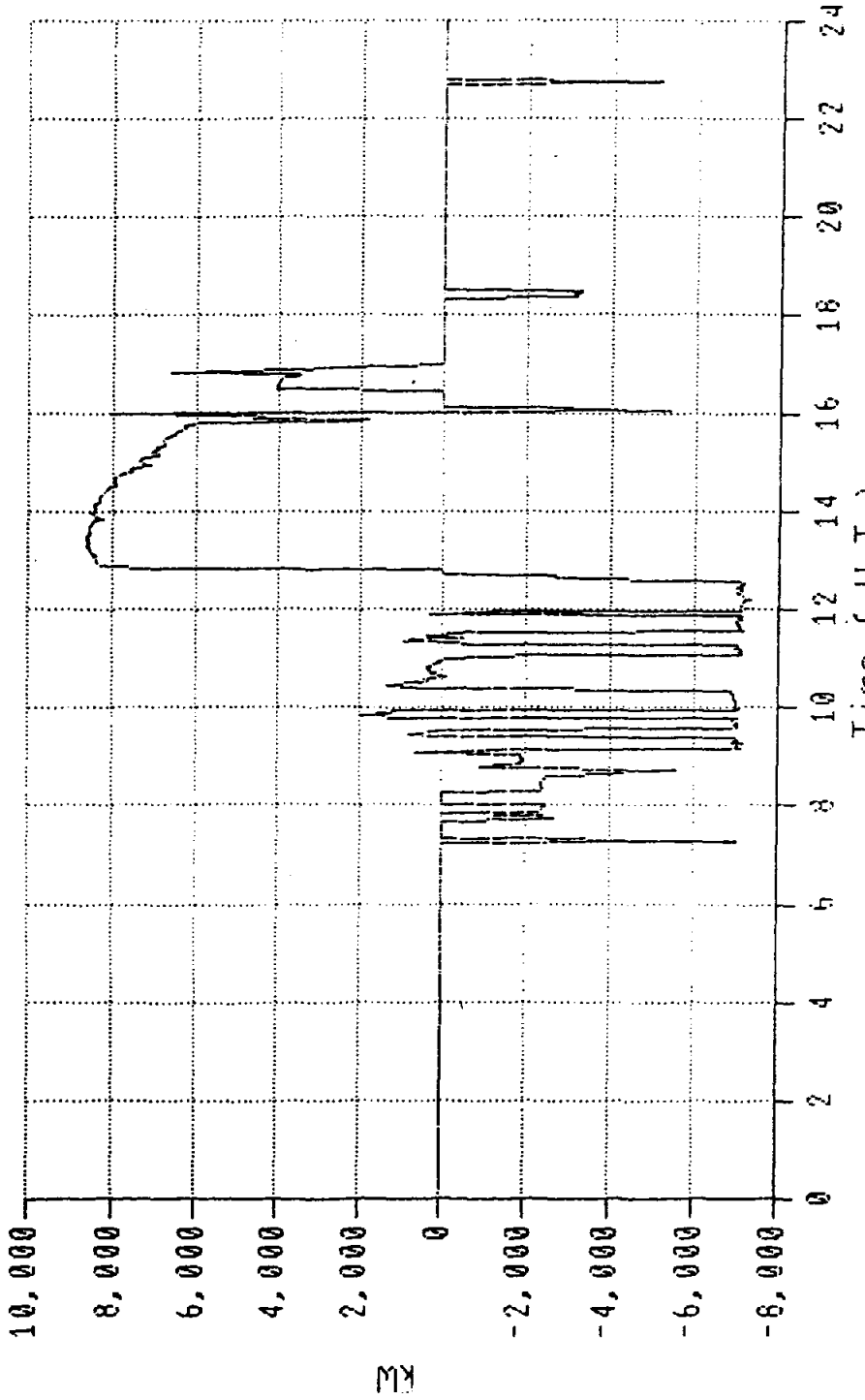

FIG 22 : THEMIS, MARCH 6, 1985 , HEAT TRANSFERRED TO THE HOT TANK

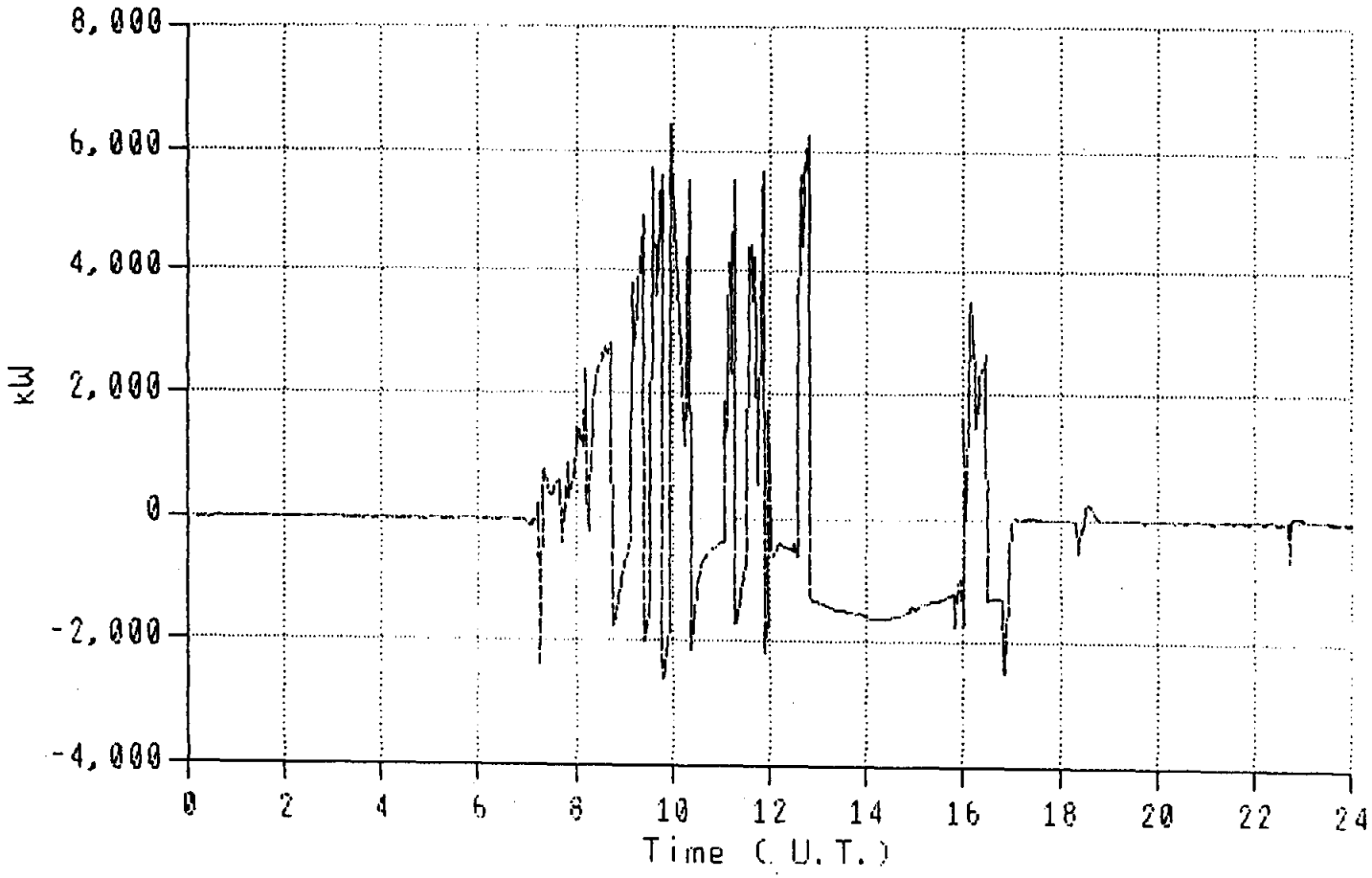

FIG 23 : THEMIS, MARCH 6, 1985 . HEAT TRANSFERRED TO THE COLD TANK

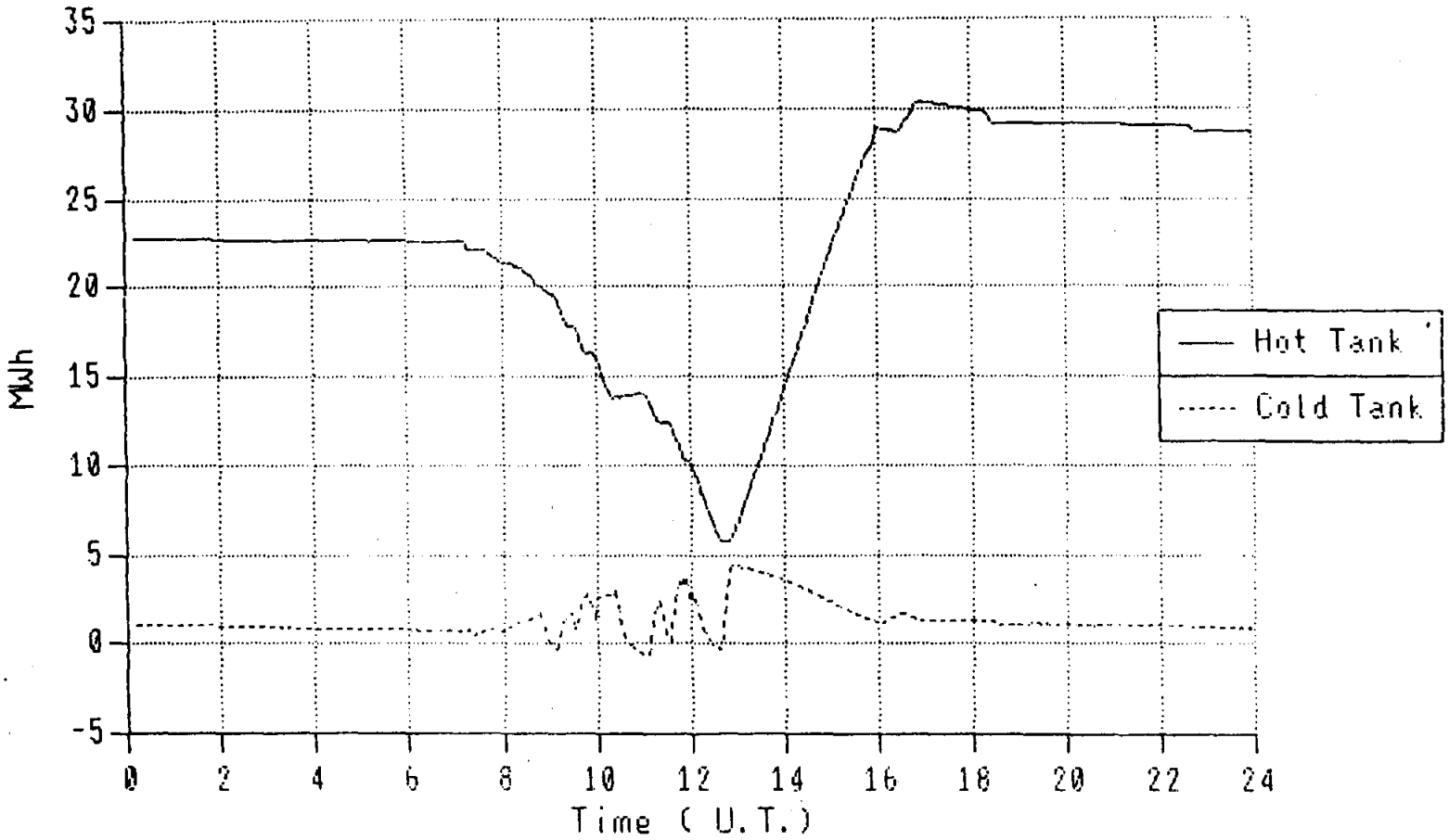

FIG 24 : THEMIS, MARCH 6, 1985 . STORED ENERGY IN THE STORAGE TANKS

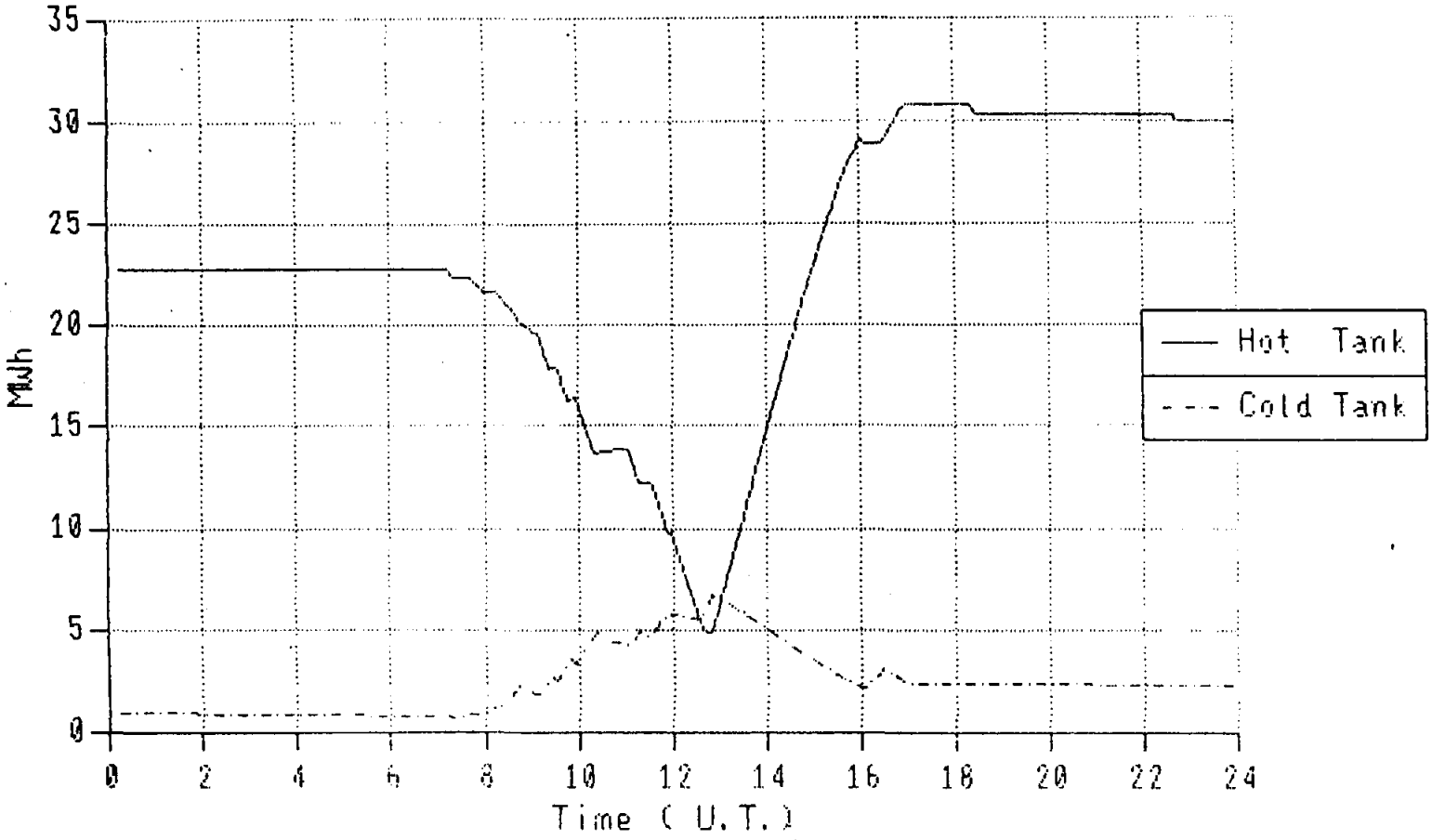

FIG 25 : THEMIS, MARCH 6, 1985 . STORED ENERGY IN THE STORAGE TANKS (CALCULATED BY THE FLOW RATE METHOD)

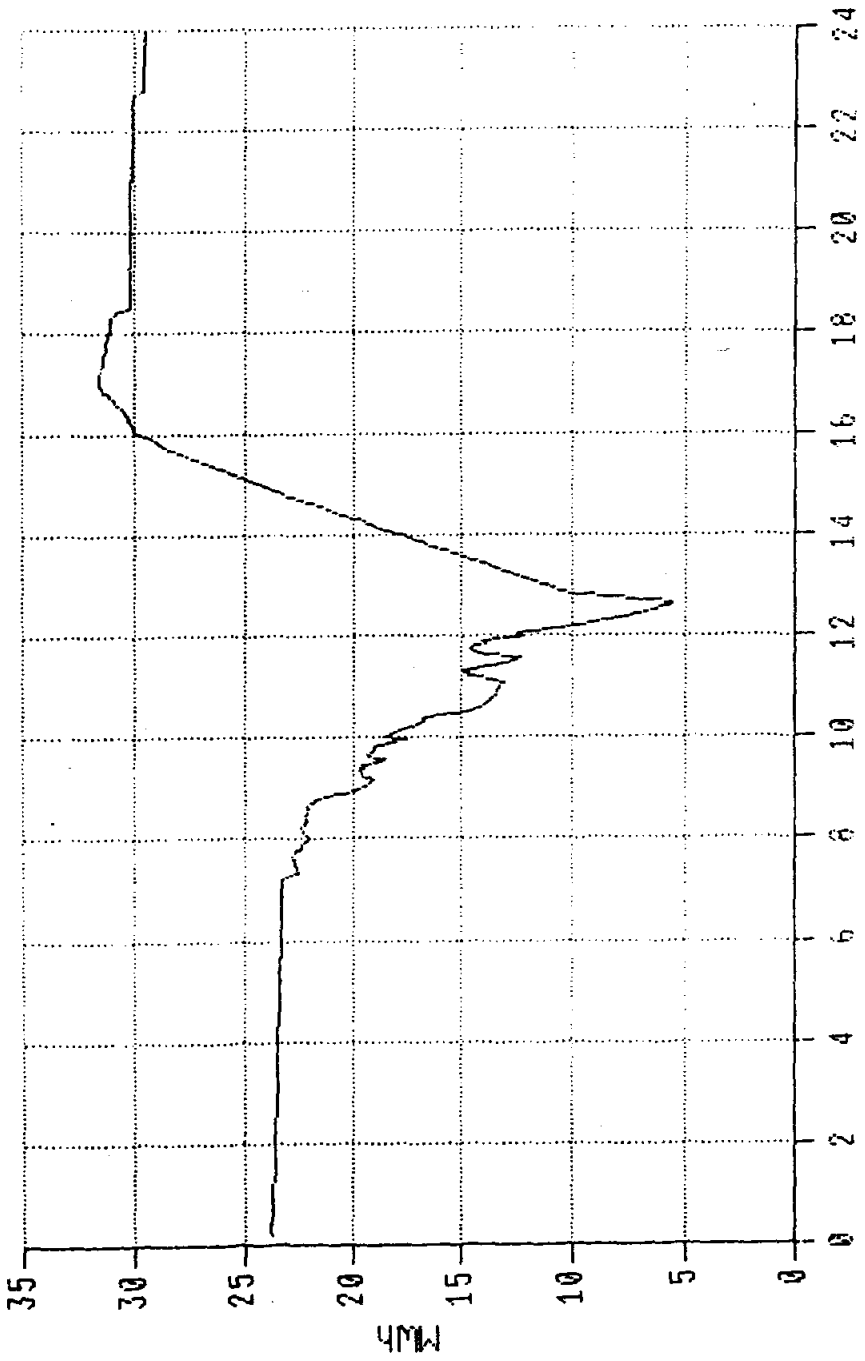

FIG 26 : THEMIS, MARCH 6, 1985 . TOTAL ENERGY STORED IN THE TWO TANKS

8.0 THERMAL STORAGE SUBSYSTEM EFFICIENCY

In this section the thermal storage subsystem efficiency is evaluated with the following assumptions :
The thermal storage subsystem is charged and discharged once a day at full capacity.
The temperature of the hot tank is 450°C and the temperature of the cold tank is 250°C.

Under these conditions. the main contributions to the thermal storage heat loss over 24 hours are:

Hot tank heat loss (55kW)	1320	kWh
Cold tank heat loss (15.2kW)	365	kWh
Hot pipe (Hot tank Steam Generator)heat loss	70	kWh
Cold pipe (Steam generator Cold tank)heat loss	20	kWh
Total thermal storage heat loss over 24 hours	1775	kWh

The thermal storage efficiency for a daily 40.000 kWh charge- discharge cycle is then :

$$\eta = 1 - 1775/40000 = 95.5\%$$

9.0 ENERGY USED TO ACTIVATE THE THERMAL STORAGE SUBSYSTEM

This section presents an evaluation of the heat investment necessary for activating the thermal storage subsystem. The plant will be assumed to be in a steady state regime at design parameters; the thermal storage subsystem will be considered empty but activated, i.e. preheated to the design temperature.

In this situation all the salt is in the cold tank at the reference temperature of 250°C. The hot tank is at the design temperature of 450°C and is empty of salt . The available energy from the thermal storage subsystem is obviously zero, but there is an appreciable amount of heat used to preheat the salt and the two tanks up to their operating temperature. The evaluation of the heat investment for activating the thermal storage subsystem is presented in Table 9-1.

The total amount of heat for activation is estimated to 67605 kWh and represents about 8.5 hours of operation of the solar receiver at the design power.

Most of this heat (91.8%) is used for melting and preheating the salt up to 250°C.

TABLE 9-1

HEAT USED FOR ACTIVATION OF THE THERMAL STORAGE SUBSYSTEM

	Mass (kg)	Specific Heat (kWh/kg°C)	Temperature (°C)	Heat Used For Activation (kWh)
Hot tank				
Vessel	40000	$1.5x10^{-4}$	450	2702
Pumps	3000	$1.5x10^{-4}$	450	202
Insulation	12000	$2.3X10^{-4}$	450-33	650
Cold tank				
Vessel	40000	$1.5x10^{-4}$	250	1500
Pumps	3000	$1.5x10^{-4}$	250	112
Insulation	12000	$2.3x10^{-4}$	250-25	345
		Solid State $3.72x10^{-4}$	20-140	23972 (Solid)
Salt	537000		melting 140	12487 (melting)
		Liquid State $4.34x10^{-4}$	140-250	25637 (liquid)

Total heat invested for activation of the thermal storage subsystem : 67605 kWh
Heat invested for melting and preheating the salt up to 250°C : 62096 kWh (91.8% of total).

10.0 INFRARED THERMOGRAPHY OF THE THERMAL STORAGE TANKS

The two thermal storage tanks and the piping were inspected for heat loss by infrared thermography in January 1984.

The equipment used was an InfraRed AGA Camera type 782. The I.R images were tape recorded and then analyzed with a magnetoscope.

The conclusions of this inspection are the following :

- Cold storage tank (FKH001BA)
  - Average external temperature of the heat insulator : 28°C.
  - Ambiant air temperature : 21°C.
  - No hot zone detected.
  - Normal behaviour of the insulation.
- Hot storage tank (FKH002BA)
  - Average external temperature of the insulation : 27°C.
  - Ambiant air temperature : 21°C.
  - No hot zone detected.
  - Normal behaviour of the insulation.
- Salt pumps FRS001PO and FRS002PO
  - Ambiant air temperature : 25°C.
  - Average temperature of pump housing : 30 to 35°C.
  - Hot zones detected at connecting flanges. Measured temperature : 60°C.

  Improvement of the insulation at the hot zones was recommended.

11.0 MAINTENANCE EXPERIENCE

The general behaviour of the thermal storage subsystem during the past two years was very satisfactory.

Nevertheless several maintenance interventions were necessary in order to keep the salt loop in service. Most of the failures were due to components interfacing the thermal storage subsystem with the receiver subsystem or with the steam generator.

The salt component failures can be summarized as follows :

Salt pumps

Many interventions are recorded for salt pump maintenance :

- Bearing inspection of FRS001PO
- Pump motor air filter cleaning FRS001PO.FRS002PO
- Pump motor brushes control FRS001PO.FRS002PO
- Salt solidification in the check valve of FRS002PO
- Salt leak at the flange gasket of FRS002PO
- Bearing repair of FRS001PO
- Bearing lubrication failure on FRS002PO. The failure was due to the breaking of a lubricating salt pipe.
- Salt pump binding (FRS002PO)
- Bearing problems on FRS002PO : breaking of connecting flange, lower bearing, shaft fastening.
- Bearing problem on FRS001PO
- Upper shaft broken on FRS002PO

Salt piping

- Heat bridges at various places of the downcomer causing cold sections and salt plugging.
- Pressurized water leak causing a deterioration of the insulation and therefore a cold section in the salt pipe connecting the steam generator to the cold storage tank. This resulted in the formation of a salt plug.
- Salt piping sliding support binding, thus inhibiting normal thermal expansion of the riser and of the downcomer.
- Leakage problems at various points of the salt loop. Generally the leaks appeared at the flange gaskets of piping and salt valves connections.

Fire problems

Hot salt leaks on electric cables started fires that destroyed the cable coverings. Similar problems occured with wooden objects and other organic materials.

Trace heating

- Trace heating pressurized water leaks under the salt pipe insulation were resposible for insulation degradation and salt pipes cold sections format

- Flanges and pipe supports were also responsible for heat bridges and salt pipes cold sections formation.

Salt flowrate measurements

Two types of salt flow rate measurements were used :

- The Venturi nozzle system which delivered excellent reliable measurements.
- The ultrasonic flowmeters which several times delivered suspicious indications and needed periodical verifications.

Lessons learned

From the above list of problems some recommendations can be expressed for future projects using salt technology :

Salt pumps

- Special attention should be given to the design of the bearings and of the supports. to avoid vibrations. lubrication problems and shaft breakage.
- It seems important to provide a small salt flow rate capability either for hot shutdowns or receiver operation at low energy input. The present lower limit at 20% of the design flowrate is too high.

Salt piping

- Salt leaks could be avoided by rejecting the principle of flanges and gaskets at pipes and valves connections. Welded sealings are more reliable and preferred.
- Heat bridges and cold salt pipes sections can be avoided by a special design of the pipe supports. by suppression of flanges. by improving the heat insulation at the salt valves and other singularities in the salt loop.
- Special care should be taken with the trace heating systems. Hot spots can appear with electric trace heating as a result of nonuniform electric heating element distribution along a salt tube. Electric contacts of the heating elements with the pipes can also create short circuits and hot spots that can melt the elements and (or) corrode a hole in the salt pipes.Pressurized water leaks were responsible for insulation degradation. Again the elimination of flanges and gaskets will reduce the leak probability. Welded seals are always preferred.
- Dismountable insulation design is recommended for allowing simpler and faster maintenance interventions.
- Service platforms are very desirable everywhere maintenance operation might be required. An example is at the top of the thermal storage tanks for allowing salt pump inspections.
- It is possible to avoid salt fires and electric cable-covering destruction by an appropriate design of the plant. The salt piping should never be placed close to the electric wires path. If some crossing points are necessary. the electric cable should be above and not below the salt components.

12.0 CORROSION

The problems of salt stability and corrosion resistance of circuit materials in the THEMIS power plant have been discussed by Spiteri in reference [7]. The types of steel selected for the salt equipment of the plant appear to be appropriate and no evidence of serious corrosion problems was reported by the THEMIS operation and maintenance team during the past two years.

The types of steel used in THEMIS equipments are the following :

Equipment	Working temperature	Type of steel
Hot storage tank FRS002BA	450°C	15CD-2-05 (AISI 4023-03MO)
Cold storage tank FRS001BA	250°C	carbon steel (A42CP)
Riser	250°C	0.5Cr-0.5MO
Downcomer	450°C	0.5Cr-0.5MO
Receiver tubes	500°C	Z3CND 17-12 (316-L.18-10MO)
Receiver headers	450°C	carbon steel (15D3-15MO3)

When salt plugs occured accidentally, salt pipes sections were cut off and analyzed. No measurable corrosion effect was observed on these test pieces.

The only serious corrosion problem was due to an error of the electric trace heating arrangement on some vents and drain tubes of the solar receiver. The heating elements formed loops causing hot spots where enhanced salt corrosion caused holes in the tubes. Consequently salt leaks occured in the receiver.

In order to prevent salt degradation, a nitrogen cover was permanently maintened over the salt level in the thermal storage tanks. This precaution, combined with the salt temperature limitation below 450°C had the positive consequence that no observable salt degradation occured in the past two years. This is confirmed by periodic salt freezing tests which showed no appreciable variation of the salt solidification temperature since the beginning of the plant experimentation.

13.0 CONCLUSIONS

One of the major technical options of the THEMIS project was the choice of the molten salt technology. This choice was motived by the wish to achieve a plant equipped with a high performance thermal storage subsystem.

After three years of plant operation, several conclusions can be drawn out.

The molten salt thermal storage concept has proved an efficient, practical, relatively reliable, and economical solution.

13.1 EFFICIENT

- A hot tank storage temperature of 415°C has been currently tested without any problem. No evidence of any limitation preventing operation at a salt temperature of 450°C, has been observed until now. Though not yet demonstrated, the operation of this thermal storage at 450°C seems achievable. At this high temperature level, this thermal storage concept can be used in connection with a high efficiency steam conversion cycle.
- The heat losses of the thermal storage tanks and piping are reasonably low, leading to a thermal storage efficiency of 95% for a daily complete charge discharge mode.
- Overnight the hot tank temperature decay doesn't exceed 3°C/12h when half full, with a salt temperature of 330°C. The temperature decay is of 18°C/12h when 5% filled at 305°C. The temperature decay would be of 2.6°C/12h when full at 450°C.

13.2 PRACTICAL

This thermal storage concept has proved the possibility of a complete decoupling between sun shining and electricity production. This results in a high degree of adaptability to a large variety of meteorological and electricity production conditions.

This type of thermal storage if connected with a molten salt receiver, enables the use of low solar flux, which means the possibility of energy collection early at sunrise and late at sunset.

On the other side, this storage allows electricity production at any time, by day or by night according to the demand.

In addition this thermal storage proved a very practical heat source for the auxiliary needs of the plant.

13.3 RELIABLE

During the three years of operation, no storage outage stopped the plant. Nevertheless several maintenance problems show that a real research and development effort should be undertaken in order to develop optimized and longer life components such as salt pumps, bearings, valves, gaskets and trace heating equipment. The significant ageing of the salt pumps after three years justifies the choice of duplicating this crucial equipment in order to guarantee its availability. It also points out the need to take a special care in the choice of these components for an eventual next project.

Moreover, for the whole salt loop, including the trace heating equipment, the THEMIS experience shows that a great attention should be given to the component specification and to the quality control at each level from the component fabrication to the onsite assembly. This is a fundamental key to the project success.

13.4 ECONOMICS

For a 200°C temperature variation (250°C/450°C), the salt enthalpy change is of 314 kJ/kg (0.087 kWh/kg). In the case of THEMIS the salt cost was 5.3 F.F/kg or $ 0.67 per kg in 1984 currency. This cost would likely be less for larger quantities.

The cost of salt was thus of 61 F.F or $ 7.6 per kWh of thermal storage capacity.

The whole storage system (storage tanks, salt, hot pumps, piping, valves, heat insulator, trace heating) with a cost of 14.6 MF.F or M$ 1.8 (1984 currency) represents only 4.9% of the total plant cost.

In addition it should be pointed out that no major problems have been identified that would limit the extrapolation of the molten salt technology to larger thermal storage systems. Very large salt tanks, typically 10000 m^3 or more, seem feasible, with internal insulation and membrane walls. The scaling laws are favorable to larger thermal storage systems from the point of view of both energy efficiency and economics.

Finally it can be noted that the molten salt technology for thermal storage application might be interesting to be used in connection with alternate heat transfer fluids. There are, for instance, arguments for considering high performance heat transfer fluids such as sodium in the receiver loop. The obvious interest in this solution would justify some research and development effort on the compatibility of these fluids in heat exchangers.

APPENDIX A. HOT TANK COOL-DOWN EXPERIMENTS.

Records of measurements of November 16,1984 and January 11,1985

There are more available records from these series of experiments. For more information. please contact the authors at Ecole Centrale.

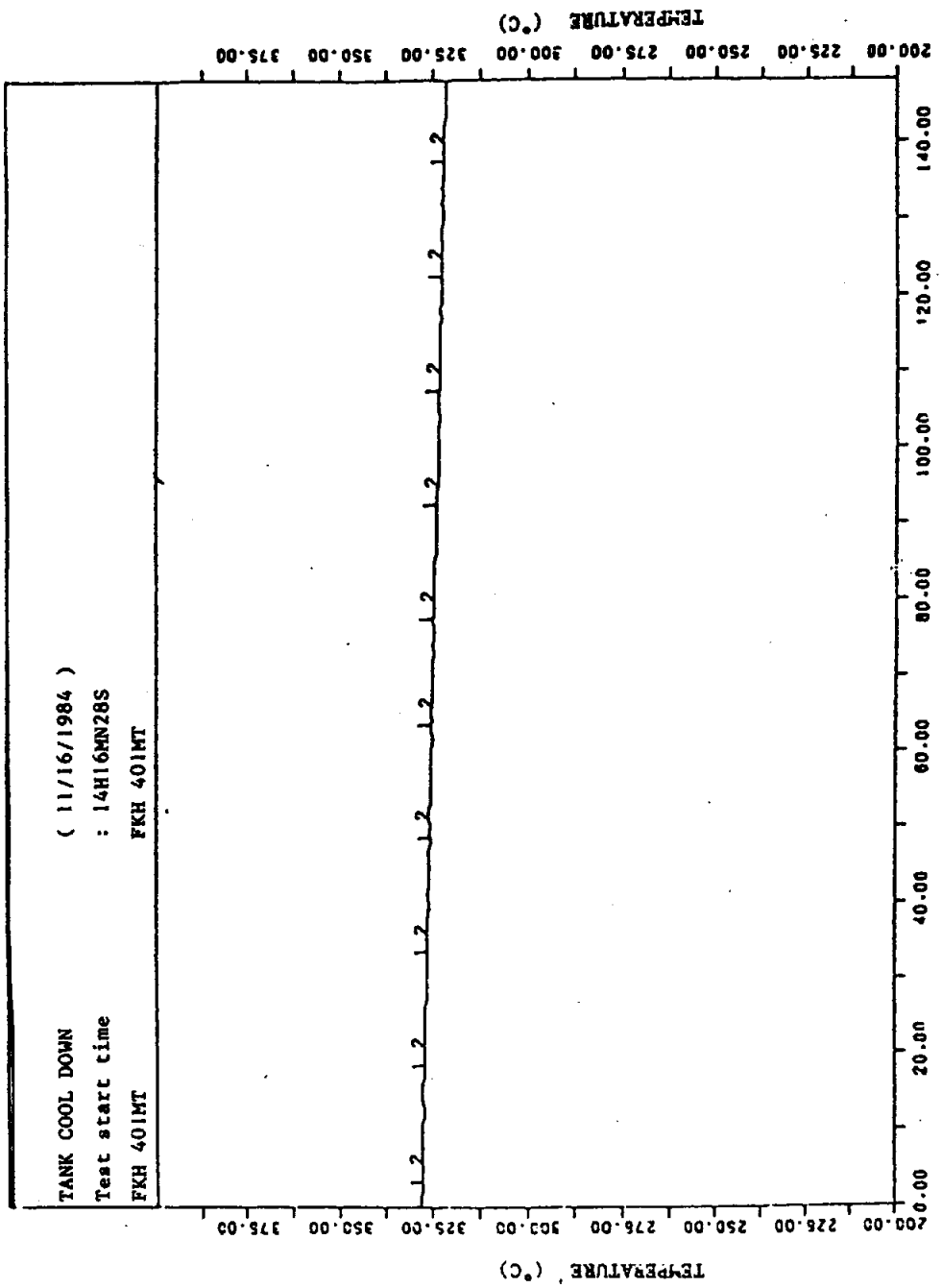

FIG 27 : THEMIS , NOVEMBER 16, 1984 , HOT TANK COOL-DOWN EXPERIMENT. SALT TEMPERATURE VERSUS TIME

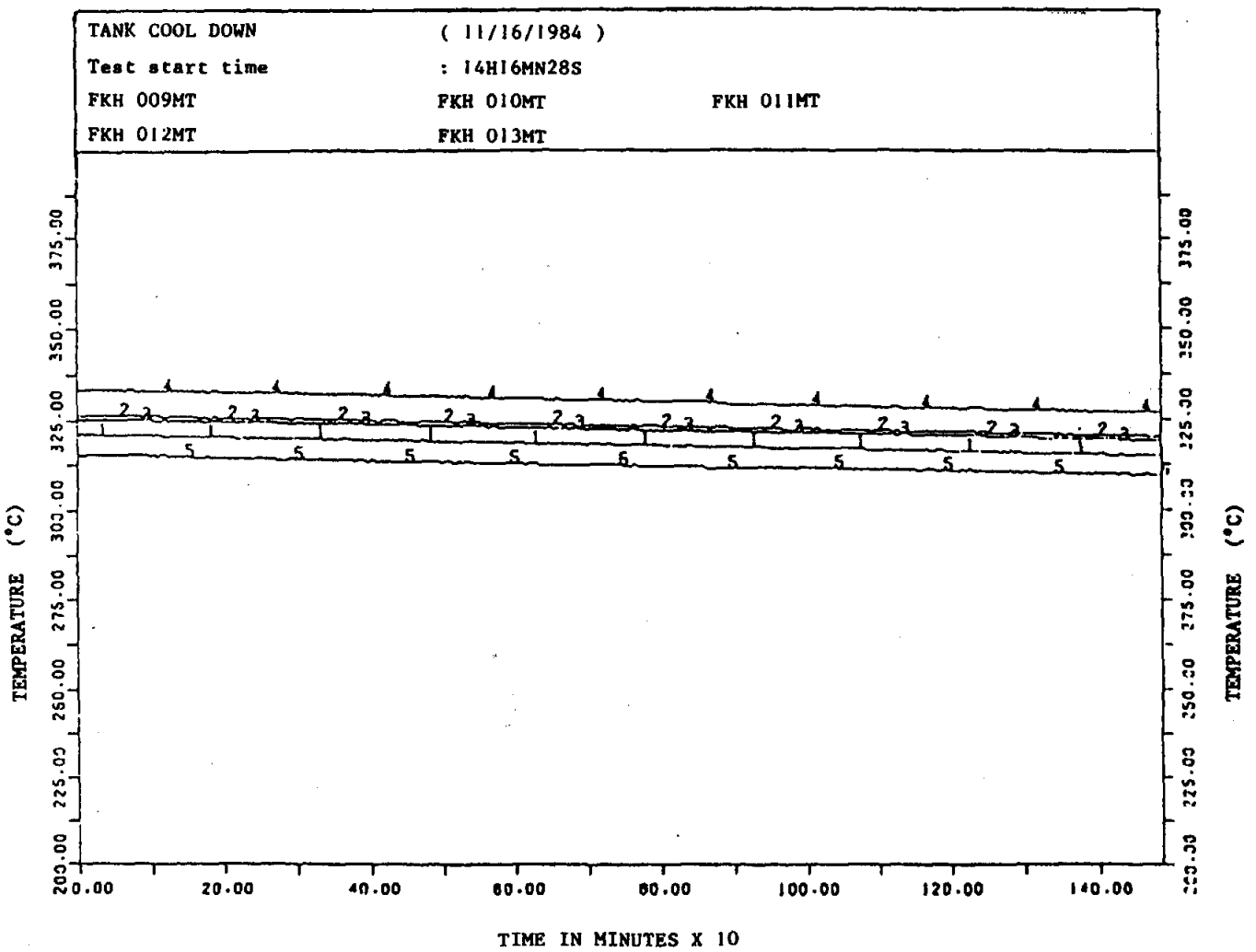

FIG 28 : THEMIS , NOVEMBER 16, 1984. HOT TANK COOL-DOWN EXPERIMENT. METAL TEMPERATURE VERSUS TIME

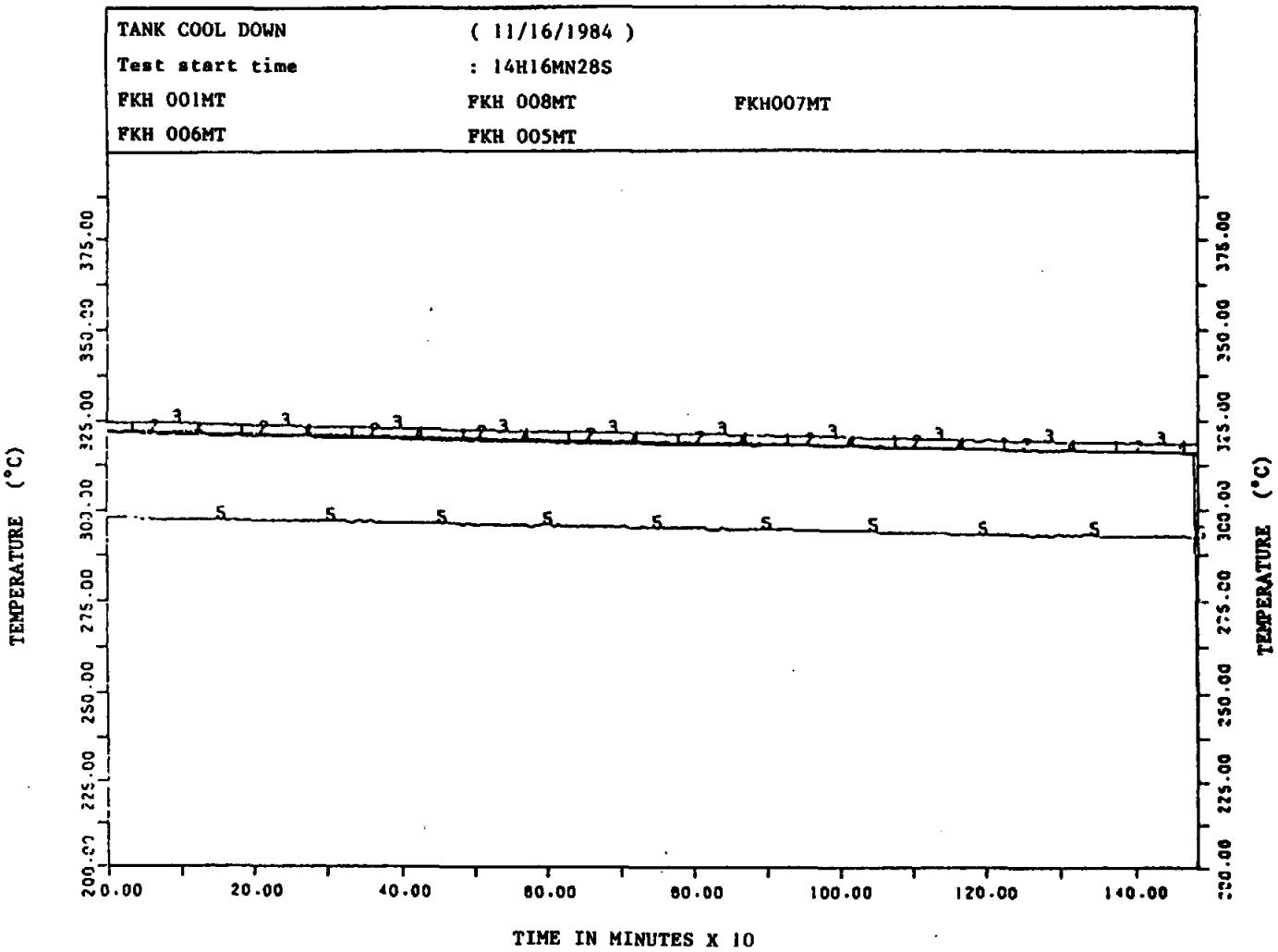

FIG 29 : THEMIS, NOVEMBER 16, 1984. HOT TANK COOL-DOWN EXPERIMENT. METAL TEMPERATURE VERSUS TIME

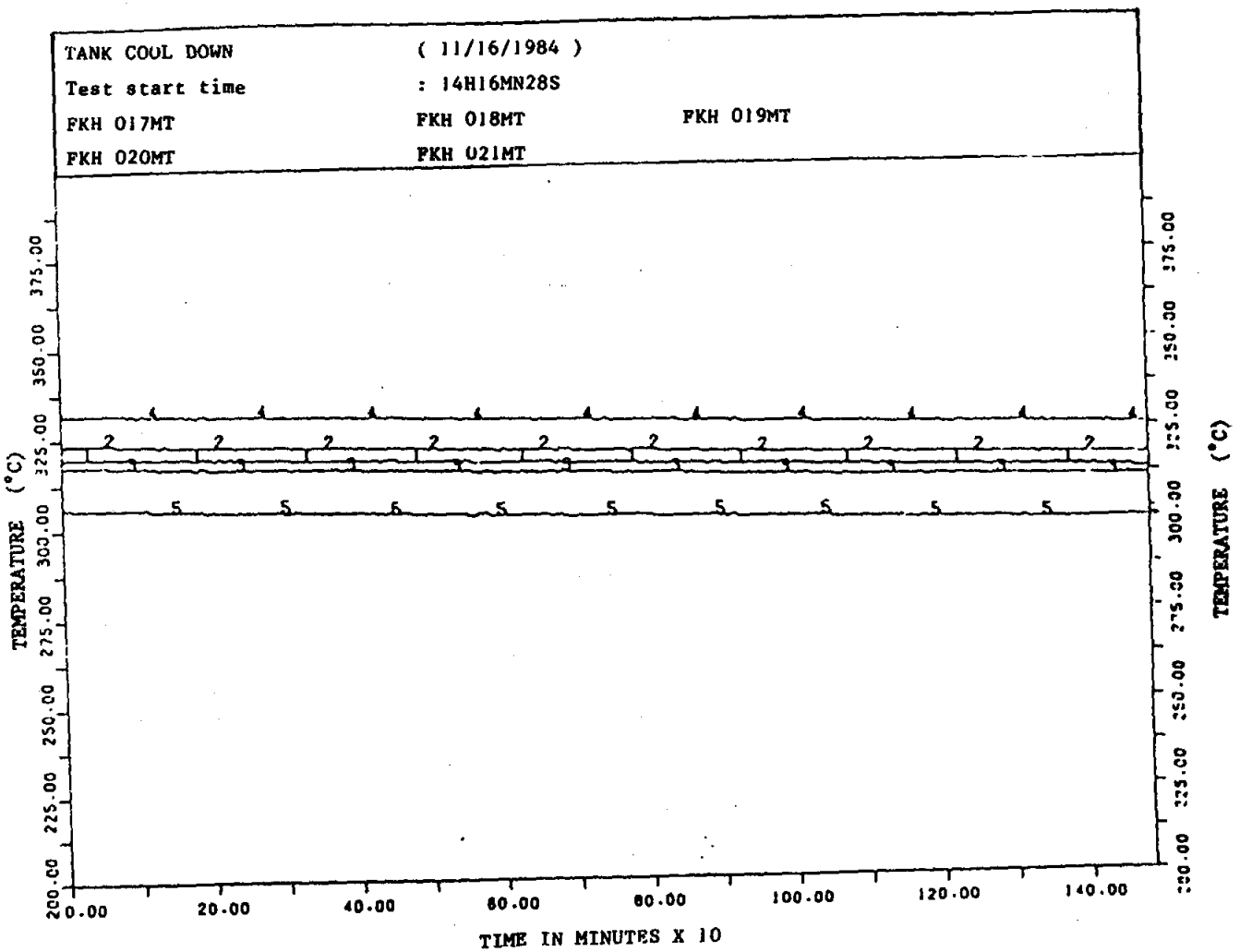

FIG 30 : THEMIS, NOVEMBER 16, 1984. HOT TANK COOL-DOWN EXPERIMENT. METAL TEMPERATURE VERSUS TIME

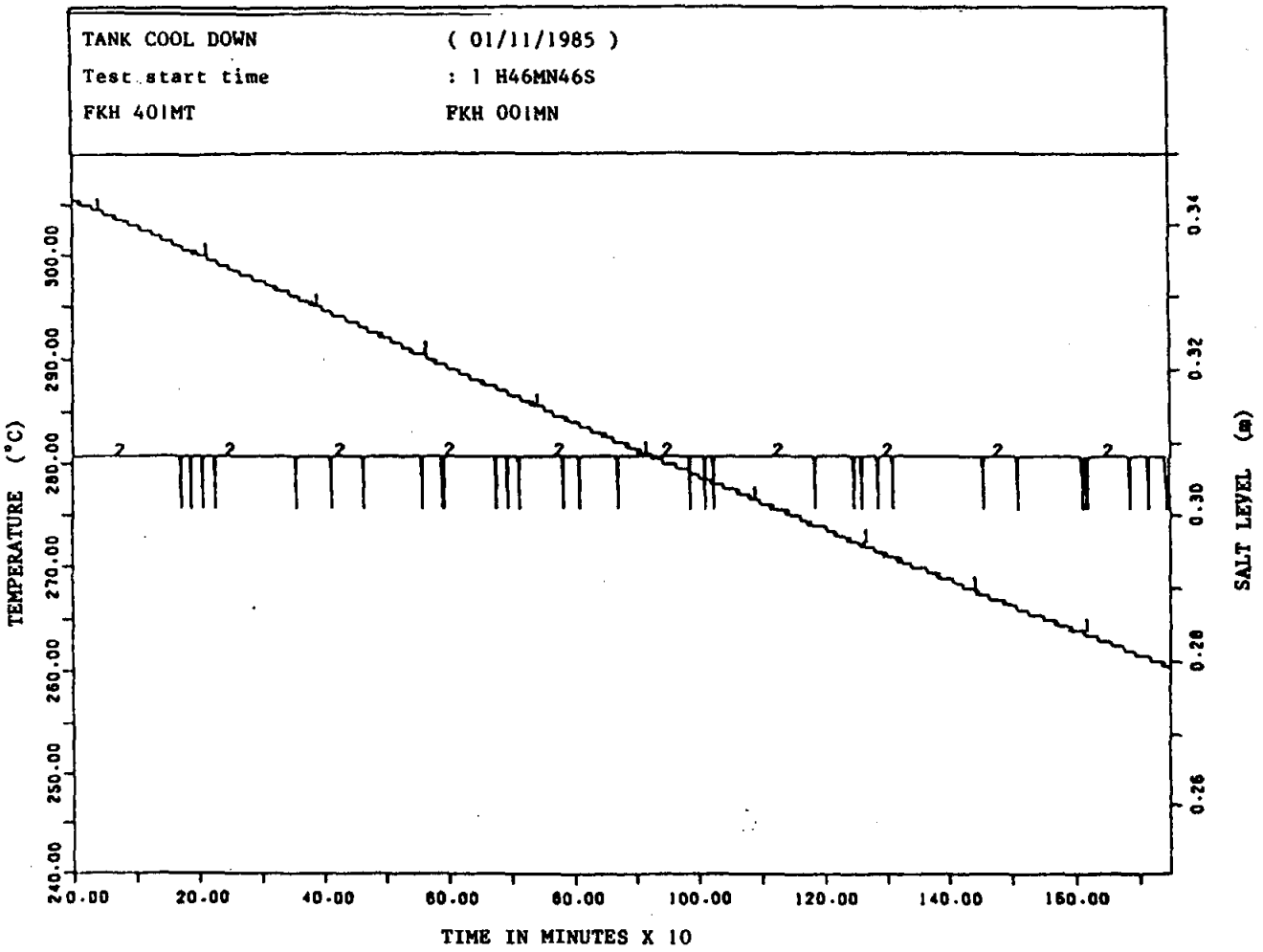

FIG 31 : THEMIS, JANUARY 11, 1985. HOT TANK COOL-DOWN EXPERIMENT. SALT LEVEL AND SALT TEMPERATURE VERSUS TIME

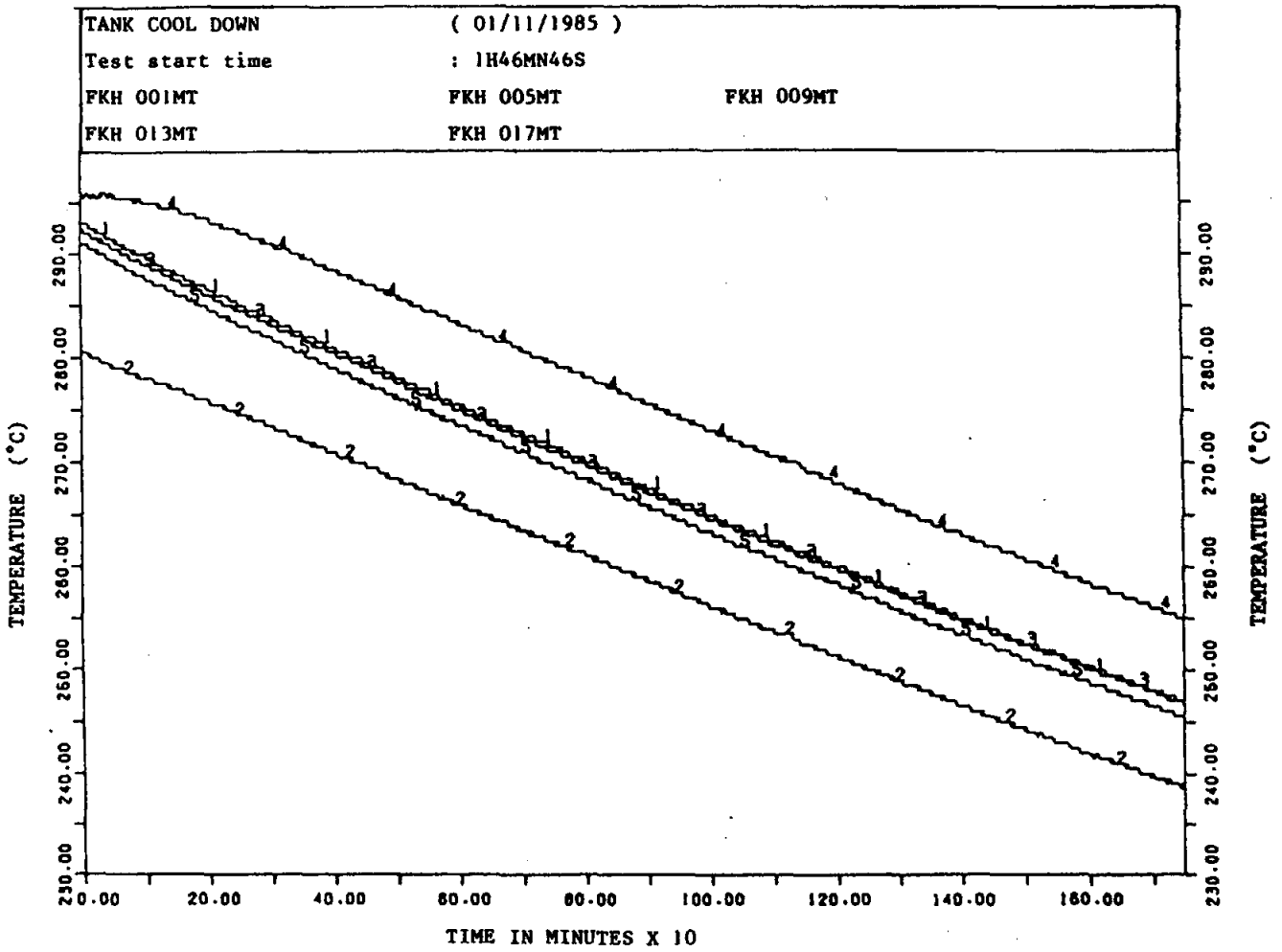

FIG 32 : THEMIS, JANUARY 11, 1985, HOT TANK COOL-DOWN EXPERIMENT, METAL TEMPERATURE VERSUS TIME

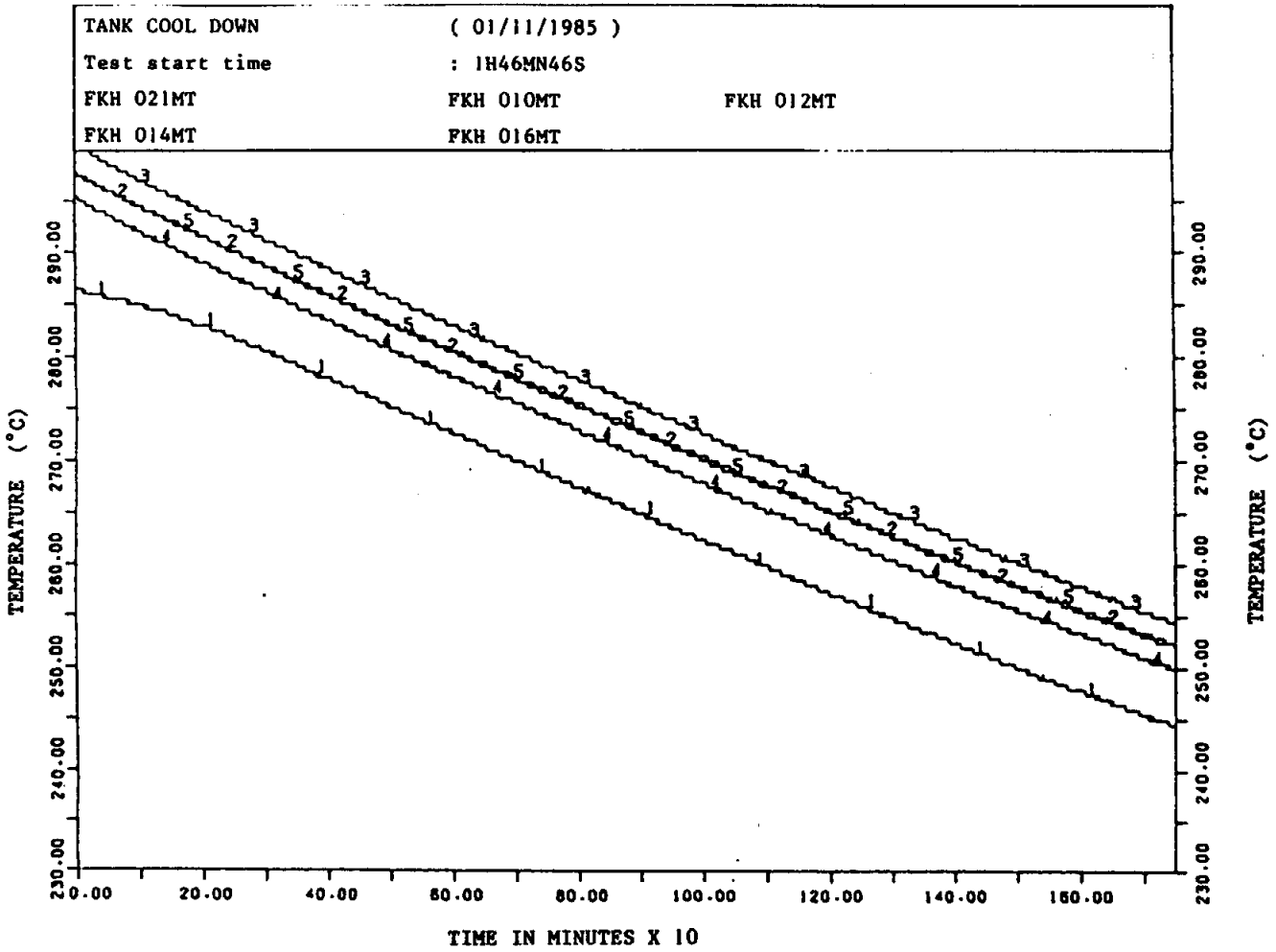

FIG 33 : THEMIS, JANUARY 11, 1985. HOT TANK COOL-DOWN EXPERIMENT. METAL TEMPERATURE VERSUS TIME

UNLIMITED RELEASE
INITIAL DISTRIBUTION

U. S. Department of Energy (5)
Forrestal Building
Code CE-314
1000 Independence Avenue, S.W.
Washington, D.C. 20585
Attn: H. Coleman
S. Gronich
F. Morse
M. Scheve
R. Shivers

U.S. Department of Energy
Forrestal Building, Room 5H021C
Code CE-33
1000 Independence Avenue, S.W.
Washington, D.C. 20585
Attn: C. Carwile

U.S. Department of Energy
Albuquerque Operations Office
P.O. Box 5400
Albuquerque, NM 87115
Attn: D. Graves

U.S. Department of Energy
San Francisco Operations Office
1333 Broadway
Oakland, CA 94612
Attn: R. Hughey

University of California
Environmental Science and Engineering
Los Angeles, CA 90024
Attn: R. G. Lindberg

University of Houston (2)
Solar Energy Laboratory
4800 Calhoun
Houston, TX 77704
Attn: A. F. Hildebrandt
L. Vant-Hull

Analysis Review & Critique
6503 81st Street
Cabin John, MD 20818
Attn: C. LaPorta

Arizona Public Service Company
P.O. Box 21666
Phoenix, AZ 85036
Attn: E. Weber

Babcock and Wilcox
91 Stirling Avenue
Barberton, OH 44203
Attn: D. Young

Bechtel Group, Inc.
P.O. Box 3965
San Francisco, CA 94119
Attn: P. DeLaquil
S. Fleming

Black & Veatch Consulting Engineers (2)
P.O. Box 8405
Kansas City, MO 64114
Attn: J. C. Grosskreutz
J. E. Harder

Boeing Aerospace
Mailstop JA-83
P.O. Box 1470
Huntsville, AL 35807
Attn: W. D. Beverly

California Energy Commission
1516 Ninth St., M/S 40
Sacramento, CA 95814
Attn: A. Jenkins

California Public Utilities Com.
Resource Branch, Room 5198
455 Golden Gate Ave.
San Francisco, CA 94102
Attn: T. Thompson

CEA IRDI D LETI (2)
Departement D'Electronique et
d'Instrumentation Nucleiare-CEN/S
91191 Gif Sur Yvette CEDEX
France
Attn: Prof. Dr. C. Etievant

CIEMAT
Avda. Computense, 22
28040 Madrid
Spain
Attn: F. Sanchez

DFVLR RF-ET
Linder Hohe
D- 5000 Koln 90
West Germany
Attn: Dr. Manfred Becker

Ecole Centrale des Arts et Manufactures (3)
Grande Voie des Vignes
92290 Chatenay-Malabry
France
Attn: Dr. M. Izygon

Eidg. Institut fur Reaktor-Forschung
(EIR)
5303 Wurenlingen
Switzerland
Attn: Dr. P. Kesselring

El Paso Electric Company
P.O. Box 982
El Paso, TX 79946
Attn: J. E. Brown

Electric Power Research Institute (2)
P.O. Box 10412
Palo Alto, CA 94303
Attn: J. Bigger
E. DeMeo

Foster Wheeler Solar Development Corp.
12 Peach Tree Hill Road
Livingston, NJ 07039
Attn: S. F. Wu

Georgia Institute of Technology
GTRI/EMSL Solar Site
Atlanta, GA 30332

D. Gorman
5031 W. Red Rock Drive
Larkspur, CO 80118

Jet Propulsion Laboratory
4800 Oak Grove Drive
Pasadena, CA 91103
Attn: M. Alper

Los Angeles Department of Water and Power
Alternate Energy Systems
Room 661A
111 North Hope Street
Los Angeles, CA 90012
Attn: Hung Ben Chu

Martin Marietta Aerospace
P.O. Box 179, MS L0450
Denver, CO 80201
Attn: H. Wroton

McDonnell Douglas (2)
MS 49-2
5301 Bolsa Avenue
Huntington Beach, CA 92647
Attn: R. L. Gervais
J. E. Raetz

Meridian Corporation
4300 King St #400
Alexandria, VA 22302-1508
Attn: D. Kumar

Public Service Company of New Mexico
M/S 0160
Alvarado Square
Albuquerque, NM 87158
Attn: T. Ussery
A. Martinez

Olin Chemicals Group (2)
120 Long Ridge Road
Stamford, CT 06904
Attn: J. Floyd
D. A. Csejka

Pacific Gas and Electric Company
77 Beale Street
San Francisco, CA 94106
Attn: J. Laszlo

Pacific Gas and Electric Company (4)
3400 Crow Canyon Road
San Ramon, CA 94526
Attn: G. Braun
T. Hillesland, Jr.
B. Norris
C. Weinberg

Public Service Company of Colorado
System Planning
5909 E. 38th Avenue
Denver, CO 80207
Attn: D. Smith

Rockwell International
Rocketdyne Division
6633 Canoga Avenue
Canoga Park, CA 91304
Attn: J. Friefeld

Sandia Solar One Office
P.O. Box 366
Daggett, CA 92327
Attn: A. Snedeker

Science Applications International Corp.
10401 Roselle Street
San Diego, CA 92121
Attn: B. Butler

Solar Energy Research Institute (3)
1617 Cole Boulevard
Golden, CO 80401
Attn: B. Gupta
D. Hawkins
L. M. Murphy

Solar Kinetics Inc.
P.O. Box 47045
Dallas, TX 75247
Attn: J. A. Hutchison

Southern California Edison
P.O. Box 325
Daggett, CA 92327
Attn: C. Lopez

Stearns Catalytic Corp.
P.O. Box 5888
Denver, CO 80217
Attn: T. E. Olson

6000 D. L. Hartley; Attn: V. L. Dugan, 6200
6220 D. G. Schueler
6222 J. V. Otts
6226 J. T. Holmes (10)
8000 J. C. Crawford; Attn: R. J. Detry, 8200
P. L. Mattern, 8300
R. C. Wayne, 8400
P. E. Brewer, 8500
8100 E. E. Ives; Attn: J. B. Wright, 8150
J. F. Barham, 8140
D. J. Bohrer, 8160
8130 L. A. Hiles
8133 L. G. Radosevich
8133 A. C. Skinrood (3)
8244 C. M. Hartwig
8245 R. J. Kee
8535 Publications Division for OSTI (10)
8535 Publications Division/Technical Library Processes Division, 3141
3141 Technical Library Processes Division (3)
8524 Central Technical Files (3)